



Climate impacts on fished populations. Part 1: Simulating bottom-up, physiological, and fishery-induced changes in production potential

New Zealand Fisheries Assessment Report 2023/56

P. Neubauer,
T. A'mar,
M. Dunn

ISSN 1179-5352 (online)
ISBN 978-1-991120-14-4 (online)

November 2023



Disclaimer

This document is published by Fisheries New Zealand, a business unit of the Ministry for Primary Industries (MPI). The information in this publication is not government policy. While every effort has been made to ensure the information is accurate, the Ministry for Primary Industries does not accept any responsibility or liability for error of fact, omission, interpretation, or opinion that may be present, nor for the consequence of any decisions based on this information. Any view or opinion expressed does not necessarily represent the view of Fisheries New Zealand or the Ministry for Primary Industries.

Requests for further copies should be directed to:

Fisheries Science Editor
Fisheries New Zealand
Ministry for Primary Industries
PO Box 2526
Wellington 6140
NEW ZEALAND

Email: Fisheries-Science.Editor@mpi.govt.nz

Telephone: 0800 00 83 33

This publication is also available on the Ministry for Primary Industries websites at:

<http://www.mpi.govt.nz/news-and-resources/publications>

<http://fs.fish.govt.nz> go to Document library/Research reports

© Crown Copyright - Fisheries New Zealand

Please cite this report as:

Neubauer, P.; A'mar, T.; Dunn, M. (2023). Climate impacts on fished populations. Part 1: Simulating bottom-up, physiological, and fishery-induced changes in production potential. *New Zealand Fisheries Assessment Report 2023/56*. 48 p.

TABLE OF CONTENTS

EXECUTIVE SUMMARY	1
1 INTRODUCTION	2
2 METHODS	3
2.1 Bioenergetics	3
2.2 Bottom-up effects: the resource spectrum	5
2.3 Population dynamics	6
2.4 Parameters	7
2.4.1 Trait scenarios	8
2.4.2 Environmental scenarios and simulation set-up	8
2.5 Evaluating productivity changes	10
3 RESULTS	11
4 DISCUSSION	28
5 ACKNOWLEDGEMENTS	29
6 REFERENCES	30
APPENDIX A OXYGEN BUDGET	33
APPENDIX B RESULTS FOR CONSTANT CATCH SIMULATIONS	35

EXECUTIVE SUMMARY

Neubauer, P.¹; A'mar, T.¹; Dunn, M.²(2023). Climate impacts on fished populations. Part 1: Simulating bottom-up, physiological, and fishery-induced changes in production potential.

New Zealand Fisheries Assessment Report 2023/56. 48 p.

Climate influences fish stocks via direct physiological effects from changes in temperature, dissolved oxygen, and acidity. Nevertheless, concomitant impacts from indirect bottom-up and top-down effects of changing environmental factors, such as food resources and predation, may play an equally important role in determining productivity changes in marine environments. Together, direct and indirect influences can lead to changes in productivity of fish stocks, especially if stocks are unable to move in space to offset environmental shifts. Changes in productivity, in turn, interact with fisheries, which also affect the productivity of stocks through plastic, density-dependent effects such as increased growth of fish at reduced densities.

To assess the influence of climate on fish stocks, the present study developed and applied a model of individual eco-physiological response to environmental factors to derive population level outcomes. It then investigated how fished stocks respond to climate variation at various levels of fishing intensity, and how these changes interact with fishing-induced changes in productivity.

The model outcomes showed that fishing led to rapid and expected density-dependent per-capita declines in natural mortality (M) and growth (periodically faster growth and larger body size) over the period of initial depletion; there was higher average M due to age- and size-structure truncation from fishing. Climate responses were relatively small, but changed in the opposite direction to fishing for M (increasing per-capita M) and body size (smaller individuals). Increased growth rates at higher temperatures in climate scenarios further enhanced density-dependent changes from fishing. Nevertheless, the present approach also suggests that even moderate changes in environmental suitability are sufficient to offset changes determined by direct temperature impacts on focal species.

Our results suggest that climate responses of productivity parameters need to be considered in combination with density-dependent responses. For many stocks, it may not be possible to separate these processes, owing to the limitations of available data.

¹Dragonfly Data Science, New Zealand.

²National Institute of Water and Atmospheric Research (NIWA), New Zealand.

1. INTRODUCTION

As climate extremes become more frequent and average ocean temperatures slowly warm in many areas, a central question for many fisheries managers is how fisheries production and yield will be affected by these changeable and changing environments (e.g., Brander 2007, Perry et al. 2010, Moore et al. 2018, Free et al. 2019).

Fisheries yields are tightly correlated with productivity of the ecosystem (Stock et al. 2017) and the biological productivity of stocks themselves. Productivity is determined by the interplay between growth, mortality, and reproduction (Mangel et al. 2010, Mangel et al. 2013, Kindsvater et al. 2016). All of these components of population productivity are determined by the physiology of the individuals that make up the population, and by their interaction with the environment (Neubauer & Andersen 2019); for example, increased metabolic needs under elevated temperatures can lead to increased foraging and “risk taking”, leading to elevated mortality but faster growth. Conversely, at metabolic limits, metabolic needs may not be met by available prey, causing reductions in growth and reproduction, with increased mortality.

In addition to physiological factors impacting productivity, fishing significantly alters the ecology of fish species by reducing their density compared with un-fished stages. In addition, through interactions between ecology and physiology, fishing has the potential to alter responses to environmental and climate influences in fished populations compared with un-fished counterparts (Perry et al. 2010, Planque et al. 2010, Shelton & Mangel 2011).

Some interactive effects of fishing and climate are likely to be life-history specific, such as effects on migratory patterns or meta-population structure; other effects, such as reduced age and size structure, appear general across the majority of wild-capture fisheries, leading to potential loss of buffering capacity and increasing fluctuations in biomass and population structure (Planque et al. 2010, Shelton & Mangel 2011). Nevertheless, environmental and climate signals may be amplified in exploited populations, but the aggregate effect of climate on fishery production appears to be variable (Britten et al. 2016, Free et al. 2019). This variability may be related to the relative strength and direction of underlying environmental, physiological, and ecological drivers, and their interaction with fishing. In view of this variability and the complexity of interactions, developing a mechanistic understanding of these interactions provides a promising approach to build predictive capacity of environmental and climate impacts on fished populations and their management (Szwalski 2016).

Although the impact of fishing on fished populations and their response to environmental factors have been relatively well-studied (Planque et al. 2010, Shelton & Mangel 2011), the physiological effects of climate on fish populations remain subject to considerable on-going research (Brander et al. 2013, Lefevre 2016, Jutfelt et al. 2018, Lefevre et al. 2018). For example, oxygen-mediated range limits may lead to shifts or constrictions of climate envelopes (Deutsch et al. 2015), but oxygen limitation remains contested as a determinant of physiological performance within the limitations of a species or stock range (Brander et al. 2013, Lefevre 2016, Lefevre et al. 2018). Within these limitations, performance may be better explained by temperature-mediated changes in metabolism and resulting energy requirements, leading to changes in fundamental ecological rates, such as foraging and predation mortality (Holt & Jorgensen 2014, 2015, Neubauer & Andersen 2019). These changes arise naturally, assuming optimal foraging strategy under changing physiological constraints imposed by temperature; they can be used to formulate a general eco-physiological framework to describe temperature impacts on individual fish (Neubauer & Andersen 2019).

Here, the individual-based eco-physiological model by Neubauer & Andersen (2019) was scaled up to population-level responses within a stochastic environment to understand i) how a variable environment and climate influence population productivity in fished stocks and, ii) how changes in productivity are affected by fishing on populations. The model simulations were conducted within a trait-based framework to enable generalised conclusions about pathways by which interactions of climate, environment, and fishing impact population productivity. A companion study assessed the influence of these interactions on fishery assessment estimates of stock status (Neubauer et al. 2023).

2. METHODS

The general approach for the simulations is summarised as follows:

1. The eco-physiological model was built, using assumptions about individual bioenergetics and their relation to environmental and ecological factors. Stochastic elements were specified to represent natural variability, both at the individual level (e.g., in terms of individual metabolism and environmental and ecological conditions encountered) and environmental dynamics (available prey), and at the population level (recruitment).
2. Parameters for trait-based models were determined with scenarios defined for i) fishing, ii) environmental factors, and iii) species traits.
3. For each scenario, the model was run for 384 replicates, using identical realisations for all stochastic parameters across all scenarios to ensure that the scenario results were comparable.
4. The role of environmental factors and their interaction with fishing was examined using both individual simulation realisations and summaries across all simulation scenarios.

2.1 Bioenergetics

Bioenergetics operate on the individual level, with growth, reproductive output, and mortality governed by available energy. Available energy A at weight w , temperature T , and activity level τ ($A(w, T, \tau)$) is the difference between energy intake (supply; $S(w, T, \tau)$) through foraging, and energy expenditure (demand; $D(w, T, \tau)$) due to standard metabolic and activity cost ($\propto \tau$):

$$\begin{aligned} A(w, T, \tau) &= S(w, T, \tau) - D(w, T, \tau) \\ &= (1 - \beta - \varphi)f(w, T, \tau)hc(T)w^q \\ &\quad - c(T)k_s w^n - \tau c(T)k_a w, \end{aligned} \tag{1}$$

where β is the specific dynamic action (SDA, or heat increment; the energy spent absorbing and transforming food), φ is the fraction of food excreted and egested, h is maximum consumption, and q is the weight scaling for ingestion. Energy intake and metabolism scale with temperature according to an activation function $c(T)$. Standard (resting; k_s) metabolism scales with weight according to n and active metabolism (k_a) is directly proportional to weight (see a list of parameter definitions in Table 1).

Energy intake depends on the maximum consumption rate $hc(T)w^q$ and a function of τ , $f(w, T, \tau)$, the activity-dependent feeding level, which is a fraction between 0 and 1:

$$f(w, T, \tau) = \frac{\tau \gamma \Theta w^p}{\tau \gamma \Theta w^p + hc(T)w^q}, \tag{2}$$

where the feeding level is determined by activity level τ , foraging rate $\gamma w^p \Theta$ (search rate γw^p times food resource availability Θ) and maximum consumption $hc(T)w^q$, with p and q weight-scaling constants for foraging and maximum consumption.

The effect of temperature, described by $c(T)$, on metabolic rates (standard and active metabolism, and maximum consumption rate) is determined by enzymatic processes (e.g., digestion, glycolysis; Jeschke et al. 2002, Sentis et al. 2013). This effect is approximated by standard Arrhenius scaling (Gillooly et al. 2001):

$$c(T) = e^{E_a(T-T_0)/(b \cdot T \cdot T_0)}, \quad (3)$$

where E_a is the activation energy (assumed constant), T_0 is the reference temperature (such that $c(T) = 1$ at 15 °C), and b is the Boltzmann constant. Oxygen supply and demand act as a limit for activity, and provide the boundary conditions within which the bioenergetic processes function (Neubauer & Andersen 2019; see Appendix A).

Metabolic demands ($D(w, T, \tau)$) are standard metabolism (SMR; $\propto k_s w^n$), which scales with exponent $n < 1$, and active metabolism ($\propto \tau k_a w$), which scales proportional to mass owing to muscular demands scaling approximately isometrically with weight (Brett 1965, Glazier 2009), and the activity fraction.

Mortality scales with activity fraction and weight as w^{q-1} (Andersen et al. 2009, Hartvig et al. 2011):

$$M(w, T, \tau) = (\rho + \mu\tau)w^{q-1} + I \frac{-A(w, T, \tau)}{\zeta w}, \quad (4)$$

The first term is base- and activity-related mortality, whereas the second term describes starvation mortality. Base mortality at mass $w = 1$ and $\tau = 0$ is given by ρ ; that is, with no activity, and μ is the coefficient for activity-related mortality. By adjusting feeding activity τ , fish simultaneously modulate their potential food intake, mortality risk, and metabolic costs. The second term uses an indicator function I for starvation mortality that is 1 if $A(w, T, \tau) < 0$, and zero otherwise. Starvation mortality is assumed to be proportional to energy loss and inversely proportional to reserves ζ at weight w . This approach reflects the assumption that animals will adjust their foraging effort to optimise fitness given temperature and oxygen constraints.

It was assumed that activity is optimised to maximise available energy relative to mortality risk. This assumption is often referred to as “Gilliam’s rule”, and is a proxy for fitness optimisation (Gilliam & Fraser 1987, Sainmont et al. 2015):

$$\tau^* = \operatorname{argmax}_\tau \left\{ \frac{A(w, T, \tau)}{M(w, T, \tau)} \right\}. \quad (5)$$

This optimisation represents a “short-sighted” (instantaneous) fitness optimisation (i.e., it does not integrate over expected levels of environmental variation), and is considered appropriate for optimisation in stable environments (Sainmont et al. 2015).

For mature animals, the fraction of energy allotted to reproduction was assumed to be a sigmoidal function of length for a more straightforward correspondence with fishing selectivity (see below for the relationship between length and weight in the model), with an asymptote at $\varphi_{max} = 0.8$. At lengths corresponding with the asymptotic length L_∞ , most of the available energy is allocated to reproduction. The allocation was parameterised as a double exponential function in length with:

$$\varphi(w_l) = \exp(-\exp(-(0.3665129 + (l - l_{mat50})/(l_{mat95}/(2.603682)))) + \log(\varphi_{max})), \quad (6)$$

where l_{mat50} is the length at which 50% of the total potential energy ($\varphi(l_{mat50}) = 0.5 \times \varphi_{max}A(w, T, \tau)$) is allocated to reproduction, and $\varphi(l_{mat50} + l_{mat95}) = 0.95 \times \varphi_{max}A(w, T, \tau)$. Because maturation was parameterised in length, a minimum age and weight at spawning was specified. The former constraint largely served to designate spawning biomass, with any individuals above this age considered to be spawning individuals (though their contribution depended on size). The weight constraint served to ensure that fish that lose condition in the model do not contribute to reproduction.

With this formulation, the energy available for reproduction is:

$$\Phi(w_l, T, \tau) = \varphi(w_l)A(w_l, T, \tau), \quad (7)$$

and the energy available for growth is described equivalently as:

$$\Gamma(w, T, \tau) = (1 - \varphi(w))A(w, T, \tau). \quad (8)$$

The number of recruits at time t is a function of the amount of reproductive potential and reproductive efficiency (i.e., not all energy is transformed into eggs, some energy is needed for spawning and other reproductive behaviour, and for gonad maintenance). Taking ε_R as the efficiency constant and w_{egg} as the egg weight, the total reproduction for an individual of weight w is then $\varphi(w)A(w, T, \tau)\varepsilon_R/w_{egg}$. Integrating this reproduction over the total numbers at weight gives:

$$R_p(T, \tau) = \int_{w_{egg}}^{w_{max}} \frac{\varphi(w)A(w, T, \tau)\varepsilon_R}{2w_{egg}} N_w dw, \quad (9)$$

where N_w is numbers-at-weight in the population. To add early-life density dependence, a stock-recruit function (close to a Beverton-Holt function) with asymptotic maximum recruitment R_{max} was superposed that allowed simulating populations with more or less early-life density dependence:

$$R(T, \tau) = R_{max} \frac{R_p(T, \tau)}{R_{max} + R_p(T, \tau)}. \quad (10)$$

Process error can be applied to $R(T, \tau)$ for age cohort a .

2.2 Bottom-up effects: the resource spectrum

Available energy is in part determined by available resources $\gamma\Theta$, which can be interpreted as the prey encounter rate (i.e., the product of search rate and prey availability). Availability is in turn determined by the predator food preference and availability of this food. If preference is largely determined by size so that:

$$\lambda(w/w_p) = \exp \left[- \left(\ln \left(\frac{w}{w_p \eta} \right)^2 \right) / (2\sigma^2) \right] \quad (11)$$

is a dome-shaped (normal) preference in log prey weight ($\log(w_p)$) relative to predator weight with preference ratio η and width σ , then:

$$\Theta = \int_0^\infty \lambda(w/w_p) w_p (cN_w + N_{w_p}^r) dw_p \quad (12)$$

is the available resource, composed of conspecifics available (via cannibalism, scaled by c) to predation, and a resource spectrum N_w^r .

The number spectrum for the resource is described as the solution to logistic growth by weight between time step t and $t + 1$ (Hartvig et al. 2011):

$$N_{w_r}(t) = K_{w_r} - [K_{w_r} - N_{w_r}(t-1)] e^{-(r_{max} w_r^{n-1} + \mu_p(w_r))}, \quad (13)$$

where $r_{max} w_r^{n-1}$ is the weight-specific growth rate of the spectrum, and $K(w_r) = K_r w_r^{-2-q+n}$ is the weight-specific carrying capacity with exponent $-2 - q + n$ (Andersen & Beyer 2006). The predation mortality for the resource is described as:

$$\mu_p(w_r) = \int_{w_{egg}}^{w_{max}} \lambda(w/(w_r))(1-f(w))\gamma w^q N_w dw. \quad (14)$$

2.3 Population dynamics

Population dynamics are described by applying growth to the numbers-at-weight for W weight classes for each cohort, such that $N_w = \sum_a N_{w,a}$. For cohort a in time step t ,

$$N_{w,a,t} = \begin{cases} R_t, & \text{for } a = t \text{ and } w = 1 \\ 0, & \text{for } a = t \text{ and } w > 1, \end{cases} \quad (15)$$

where R_t is determined from N_w across all cohorts $a < t$. Cohorts for which $t > a$ are represented as independent “populations” according to:

$$\vec{N}_{a,t} = (\vec{N}_{a,t-1} \circ \Sigma_w) \cdot G, \quad (16)$$

where G is a $W_{max} \times W_{max}$ growth-transition matrix calculated from stochastic realisations of $\Gamma(w, T, \tau)$. Survival Σ is calculated from mortality-at-weight for each weight in cohort a (M_w) as $\exp(-M(w_a, T, \tau))$, and $\vec{N}_{a,t-1}$ are numbers-at-weight for the previous time step. The first operation is the element-wise product (Hadamard product), while the second operation is the dot product of numbers-at-weight after mortality and growth.

To represent length, a dimension l was added to the array above, so that each length had a corresponding full vector of length W .

The length-weight relationship was represented as the upper limit of weight for a given length class, so that:

$$w_l^{max} = \alpha^{weight} l^{\beta^{weight}}, \quad (17)$$

with α^{weight} and β^{weight} constant. Fixing w_l^{max} for each length implied that, at a weight greater than w_l^{max} , length growth occurs; however, if the bioenergetic balance is negative, the weight for a given length decreases (i.e., the fish loses condition).

Starting iteratively from $l = l_{min}$:

$$N_{l,a,t} = \begin{cases} I^{w \leq w_l^{max}} N_{l,a,t}, & \text{for } l = l_{min} \\ \sum_{i=1}^l I^{w_i^{max} < w \leq w_l^{max}} N_{i,a,t}, & \text{for } l_{min} > l \leq l_{max}, \end{cases} \quad (18)$$

where I is an indicator variable that is 1 when the condition in the superscript is met.

Table 1: Parameter definitions and values of the constrained activity model for two species traits: slow and fast life histories or strategies. Rates are specified per unit time t , taken to be season in the model runs. Parameters were derived from considerations described in previous studies (Andersen & Beyer 2006, Andersen et al. 2009, Andersen & Beyer 2013, Andersen et al. 2017, Neubauer & Andersen 2019). Specific dynamic action, or heat increment, the energy spent absorbing and transforming food; search rate related to the foraging rate of a predator; activation energy, is the scaling parameter for temperature related processes; MOS, maximum oxygen supply; SD, standard deviation; CV, coefficient of variation.

Description	Symbol (unit)	Value	
		Slow strategy	Fast strategy
Biomass metabolism			
Specific dynamic action	β	0.1	
Egestion and excretion	φ	0.3	
Coeff. for std. metabolism	$k_s (\text{g}^{1-n} \cdot \text{y}^{-1})$	1	1.5
Coeff. for act. metabolism	$k_a (\text{g} \cdot \text{y}^{-1})$		1.5
Exponent for std. metabolism	n	0.88	0.7
Feeding ecology			
Coeff. for search rate	$\gamma (\text{g}^{1-p} \cdot \text{t}^{-1})$	13.2	
Exponent for search rate γ	p	0.8	
Coeff. for maximum consumption rate	$h (\text{g}^{1-q} \cdot \text{t}^{-1})$	30	60
Exponent for max. consumption h	q	0.8	
Coeff. for constant mortality	$\rho (\text{g} \cdot \text{t}^{-1})$	0.05	0.2
Coeff. for activity-related mortality	$\mu (\text{t}^{-1})$	0.05	
Energy reserves	ζ	0.2	
Preference ratio mean	v	1000	100
Preference ratio SD	σ_{nu}	2	1.6
Temperature sensitivity			
Reference temperature	$T_{ref} (\text{°C})$	15	8
Activation energy	E_a		0.52
Temperature at maximum MOS	T_{max}	23	8
Temperature range	$T_{lethal}^- - T_{lethal}^+$	5–30	5–15
Maturation			
Length at 50% max. investment in gonads	$l_{mat50} (\text{cm})$	20	30
Parameter defining 95% of max. investment in gonads	$l_{mat95} (\text{cm})$	10	30
Asymptotic reproductive allocation	φ_{max}		0.8
Minimum reproductive age (weight)		3 (100g)	2 (200g)
Population			
Recruitment	$R_{max} (\text{ind.t}^{-1})$	$10^{7.9}$	10^{10}
Resource			
Resource productivity coefficient	$r_{max} (\text{t}^{-1})$	0.2	
Resource carrying capacity coefficient	$K_r (\text{ind.t}^{-1})$		10^{12}
Fishing			
Selectivity (logistic)	$l_{50} (\text{cm})$	25	30
Fishing mortality (fixed)	$F (\text{t}^{-1})$	0.1	0.4
Constant catch (mean; CV 20%)	$C (\text{tonnes})$	20 000	50 000

2.4 Parameters

The current study explored the consequences of climate, ecosystem, and fishing effects in a trait-based context to ensure a level of generality beyond existing, species-specific eco-physiological models.

2.4.1 Trait scenarios

For the trait scenarios, species were distinguished along a gradient of life history. At one end of the spectrum, productivity was prioritised, i.e., energy acquisition was at the cost of increased metabolism and mortality (henceforth called the “fast strategy”, indicated by subscript f). At the opposing end of the spectrum, mortality and metabolic costs were minimised at the expense of productivity (henceforth “slow strategy”, indicated by subscript s). This axis leads to an approximately constant ratio of productivity to mortality, and corresponds to a line of equal size in the life-history space proposed by Charnov et al. (2013). In other words, the axis distinguishes species of similar size by defensive or slow versus active life histories.

The axis was implemented here based on the result that species with a more active, productivity-oriented life history (e.g., predatory pelagic fish) have a higher standard metabolism and lower weight scaling of metabolic costs than slow-strategy species (Priede 1985, Killen et al. 2010).

It was assumed that higher standard metabolism is due to increased digestive capacity (i.e., is used for gut maintenance), though high muscle mass and a larger heart would also contribute to a higher standard metabolism in active species (Priede 1985). In practice, it was assumed that approximately 50% of the standard metabolic cost is due to supporting organs associated with feeding activity only. Based on this assumption, a doubling of the maximum ingestion leads to a 50% increase in standard metabolic cost. It was further assumed that these active species have a less effective refuge from predators and, therefore, have a higher constant mortality (i.e., $M_s(w, \tau) = (0.05 + 0.05\tau)w^{q-1}$ and $M_f(w, \tau) = (0.2 + 0.05\tau)w^{q-1}$) (see exact parameter values for the trait scenarios in Table 1). Combined, these assumed trait differences lead to considerably different ecological and bio-energetic responses of slow and fast strategists (see Neubauer & Andersen 2019), with τ^* found at lower activity levels for slow strategists.

The scenarios were parameterised to allow for excess metabolic scope beyond maximum foraging activity (i.e., $\tau = 1$). This assumption is consistent with observations that the aerobic scope often exceeds energetic requirements from swimming alone, and is adapted to provide oxygen for digestion (SDA). The oxygen demand of the latter can be as high or higher than that of locomotion alone (Priede 1985). All remaining bioenergetics and population parameters were derived from considerations described in previous studies (Andersen & Beyer 2006, Andersen et al. 2009, Andersen & Beyer 2013, Andersen et al. 2017, Neubauer & Andersen 2019).

Fishing was parameterised as fishing at constant fishing mortality rate F , with scenarios run with randomly drawn (among replicates), constant (within replicates) catch presented as a sensitivity for the results here. Both constant F and constant catch were determined empirically to lead to fishing scenarios that lead to sustainable but high exploitation (on average for constant catch). Logistic selectivity was applied to reflect fishing being slightly delayed with respect to the maturity ogive (the proportion of mature individuals at age or length).

2.4.2 Environmental scenarios and simulation set-up

Environmental scenarios were designed to reflect environmental variability at different scales. To reflect small-scale variability in environmental condition at the population level and within a time step, variability was assumed for metabolic requirements (k), resource availability (Θ), and natural mortality (M); it was expressed as realisations of a random variable at each time step.

The latter two random draws were linked, assuming that higher resource availability comes at the cost of higher mortality (i.e., it is accompanied by higher predator presence also). This assumption has the practical effect that stark fitness advantages are avoided (i.e., high resource availability and low M) in parts of the population. The coefficient of variation (CV) for k was set to 0.1, and the CV for $\Theta(M)$ to 0.4, with random variates drawn from a log-normal distribution.

The second level of variability was simulated as among-year and decadal environmental and temperature variability at the level of simulation replicates. For each replicate, auto-correlated deviations were simulated from a mean for the magnitude and productivity of available resources (i.e., the intercept K_r and r_{max} of the resource size spectrum), and allowed maximum recruitment R_{max} to follow these same trends. Temperature was simulated seasonally, with seasonal variation applied to the mean. Auto-correlated deviations from seasonal means were applied to the resulting time series as a correlated deviation related to the environment by a correlation term.

Climate scenarios were defined as the baseline (base) with no temperature or environmental change, a scenario with increasing temperature only (incr temp/const env), a scenario with increasing temperature and environmental decline (incr temp/decr env), and a scenario with increasing temperature and increasing environmental suitability (incr temp/incre env) (parameter values for environmental trends are listed in Table 2).

Environmental and habitat suitability was considered as a synonym for declines determined by bottom-up factors or increases in food availability (e.g., changes in zooplankton composition or availability). Changes in top-down controls were not explored.

A total of 200 replicates were run for a range of the four climate scenarios—the last type of variation—each with or without fishing. Each replicate used the same random seed across climate and fishing scenarios, resulting in a set of eight simulation runs per replicate (random seed) across each of the two species traits (see example in Figure 1).

Table 2: Parameter values of environmental scenarios in the simulations for two species trait scenarios, slow and fast strategy species. Base, no temperature or environmental change; incr temp/const env, increasing temperature, no environmental change; incr temp/decr env, increasing temperature, declining environment; incr temp/incre env, increasing temperature, increasing environmental suitability. SD, standard deviation; CV, coefficient of variation.

Climate scenario	Slow strategy				Fast strategy			
	Base	incr temp/ const env	incr temp/ decr env	incr temp/ incre env	Base	incr temp/ const env	incr temp/ decr env	incr temp/ incre env
Temperature								
Mean temperature			15					8
SD temperature deviations								0.2
Slope	0		0.005.t ⁻¹		0			0.005.t ⁻¹
Environment								
Autocorrelation								0.95
CV env. deviations								0.1
Temperature/Env. corr.			0.95					-0.5
Slope	0	0	-0.001.t ⁻¹	0.001.t ⁻¹	0	0	-0.001.t ⁻¹	0.001.t ⁻¹

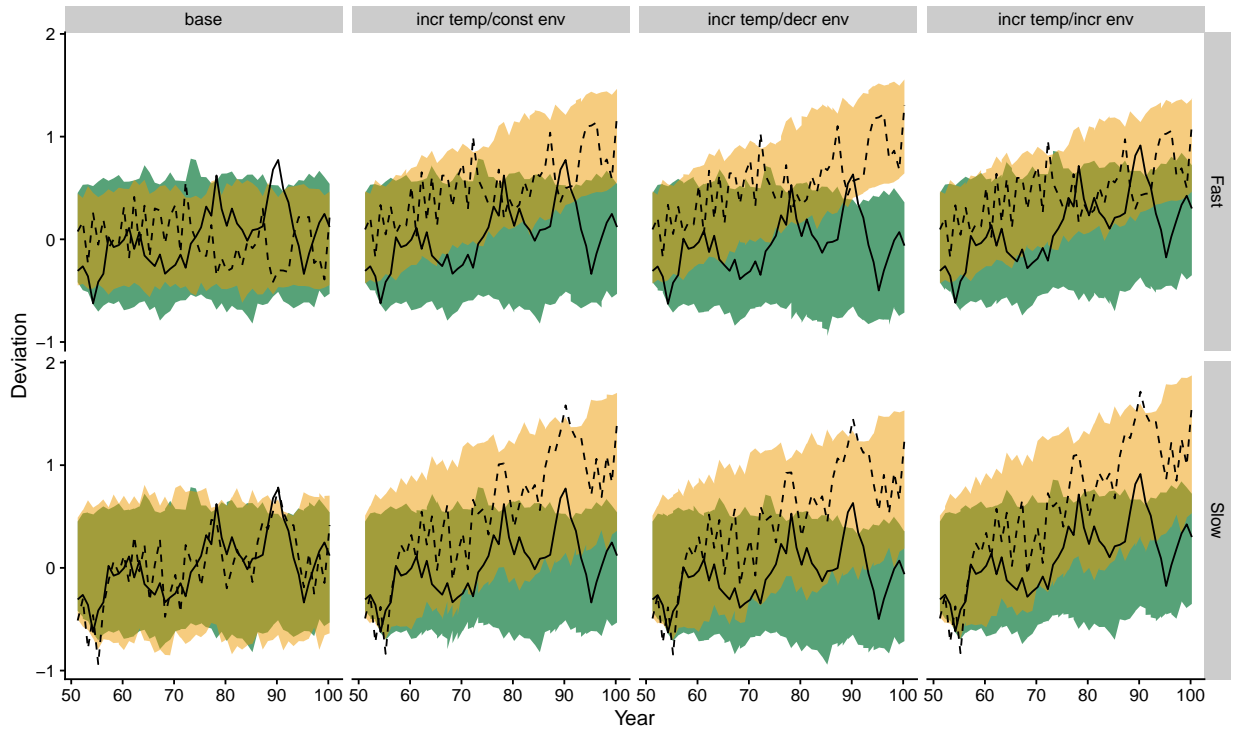


Figure 1: Simulations of different climate scenarios for fish stocks with fast (top panels) and slow (bottom panels) life-history traits. Relative environmental suitability (green) and temperature (yellow) across all simulations and for two replicates (dashed line, temperature; solid line, environmental suitability). Climate scenarios were: base, no temperature or environmental change; incr temp/const env, increasing temperature, no environmental change; incr temp/decr env, increasing temperature, declining environment; incr temp/incre env, increasing temperature, increasing environmental suitability.

2.5 Evaluating productivity changes

We evaluated productivity changes both in terms of individual productivity metrics, using natural mortality at size ($M(w, T, \tau)$) or abundance-weighted mortality at size ($1 / \sum_w N_w \sum_w M(w, T, \tau) * N_w$). To examine changes in growth, we fitted von Bertalanffy growth models to annual simulated length-at-age to provide parameter values that are more easily interpreted in terms of common fishery stock-assessment practice. In addition, we consider aggregate productivity in terms of spawners-per-recruit assuming stationary productivity parameters for all age and size classes at time t :

$$SR_t = \sum_{a,l,w} (\Pi_{a=0}^{a-1} S_{a,l,w}) \\ \Phi_{a,l,w} n_{a,l,w} / N_a.$$

3. RESULTS

The simulations provided contrasting examples between fish stocks with different life histories, even though fishing mortality was constant. Stocks with a predominantly environmentally-driven fast life history exhibited a range of depletion levels compared with slow life-history stocks that showed strong fishing-related declines and subsequent fluctuations in abundance (Figures 2 to 4). For both life histories, environmental trends for individual replicate runs led to varying trends in relative spawning biomass among replicates, including fishing and environmentally-driven declines and recoveries (e.g., see dashed lime-coloured line in Figure 2).

Climate-driven long-term trends in temperature and environmental suitability led to consistent responses relative to the base scenario: increasing temperature only led to slight declines in relative spawning stock biomass relative to the base case (Figures 2 and 3); there were more pronounced declines when environmental suitability was declining concurrently (Figure 3). When environmental suitability increased, relative spawning stock biomass increased relative to base simulations. For slow life-history stocks determined by fishing, fishing interacted with climate scenarios. This interaction produced less pronounced declines in relative spawning stock biomass based on temperature alone compared with the base case, but more pronounced increases in relative spawning stock biomass with increases in habitat suitability.

Fishing had a strong effect on all productivity parameters, leading to rapid density-dependent changes. For a simulation replicate with an initial fishing-related decline and subsequent environmentally-driven recovery (see dashed lime-coloured line in Figure 2), individual mortality risk at age (and length) declined when density was lower (Figure 5). Due to truncation of the age and size structure from fishing (Figure 6), aggregate (abundance-weighted) natural mortality at the level of the population increased initially given declining mortality with size in the present model (Figure 7). Under climate scenarios, mortality increased with temperature and declining habitat suitability, whereas increasing habitat suitability offset increases in mortality from temperature (Figure 8). These effects were more pronounced for unfished than for fished stocks. Increases in M were explained by increased foraging to offset higher metabolic cost, resulting in higher natural mortality M (Figure 9).

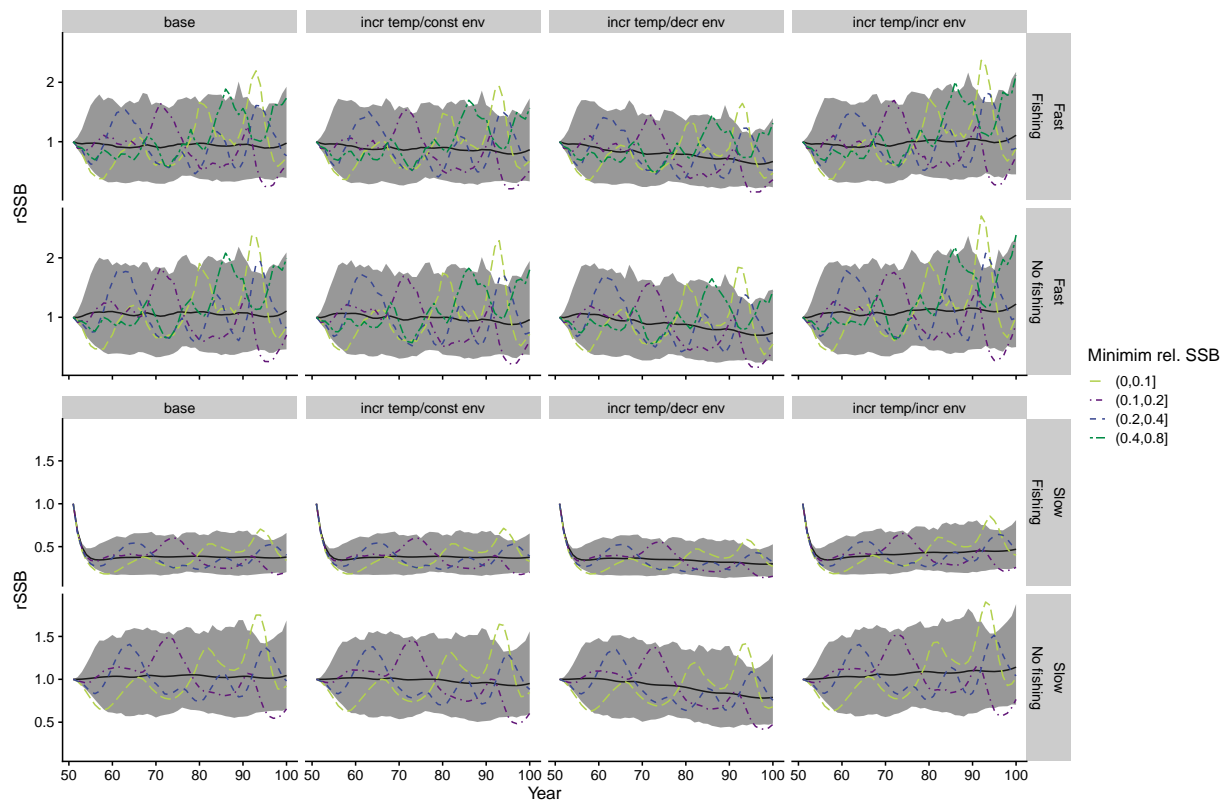


Figure 2: Trajectories of simulated relative spawning stock biomass (rSSB) for fish stocks with fast (top two rows) and slow (bottom two rows) life histories, with fishing mortality constant. Shown are the median by year (black line) and the 95% inter-quantile range of simulations (grey shaded area) with rSSB across all simulations, and randomly selected simulation replicates across levels of minimum relative stock biomass (coloured and dashed lines). Simulations were with and without fishing for four different climate scenarios: base, no temperature or environmental change; incr temp/const env, increasing temperature, no environmental change; incr temp/decr env, increasing temperature, declining environment; incr temp/incr env, increasing temperature, increasing environmental suitability.

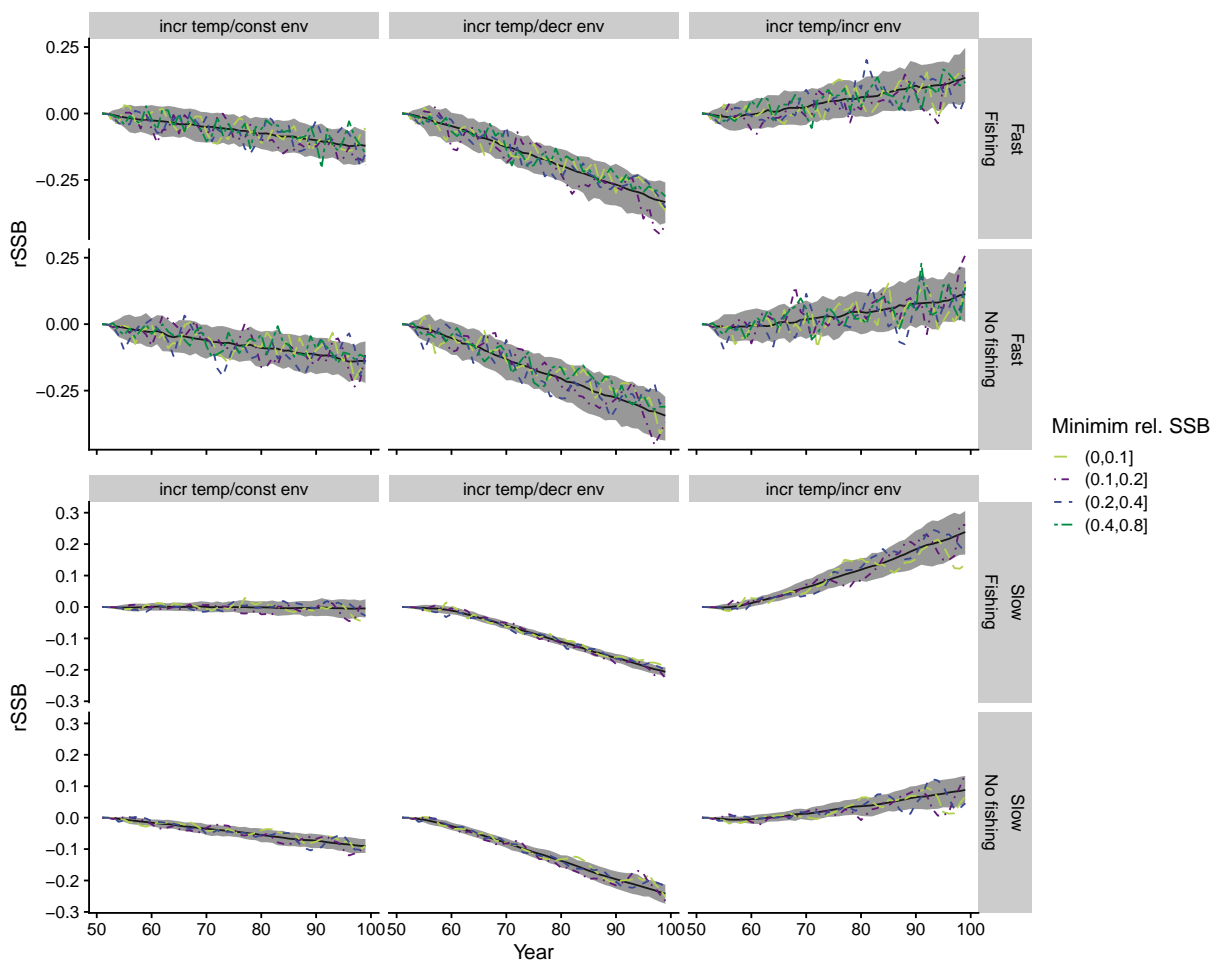


Figure 3: Trajectories of simulated relative spawning stock biomass (rSSB) relative to the base scenario for fish stocks with fast (top two rows) and slow (bottom two rows) life histories, with fishing mortality constant. Shown are the median by year (black line) and the 95% inter-quantile range of simulations (grey shaded area) with rSSB across all simulations, and randomly selected simulation replicates across levels of minimum relative stock biomass (coloured and dashed lines). Simulations were with and without fishing for three different climate scenarios, relative to the base scenario (no temperature or environmental change): incr temp/const env, increasing temperature, no environmental change; incr temp/decr env, increasing temperature, declining environment; incr temp/incre env, increasing temperature, increasing environmental suitability.

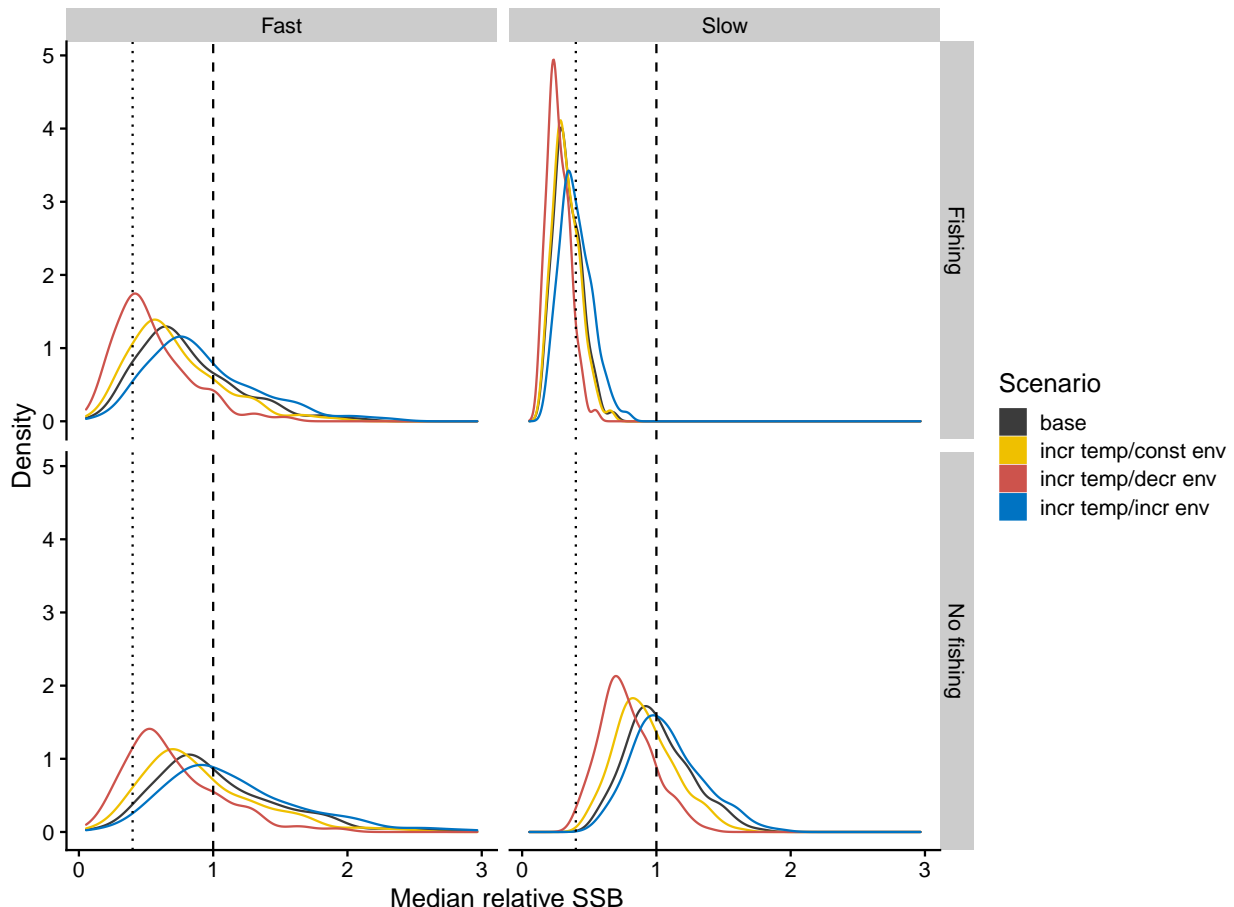


Figure 4: Simulation outcomes for stock status (relative spawning stock biomass, rSSB) for the last simulation year of the current study for fish stocks with fast (left column) and slow (right column) life histories. Fishing mortality was assumed to be constant. Simulations were with and without fishing for four different climate scenarios: base, no temperature or environmental change; incr temp/const env, increasing temperature, no environmental change; incr temp/decr env, increasing temperature, declining environment; incr temp/incr env, increasing temperature, increasing environmental suitability. All simulation replicates started from the same random seed. Dotted line indicates $0.4 \cdot SSB_0$, dashed line SSB_0 , the spawning stock biomass at year 50 (i.e., before fishing commenced for fished scenarios).

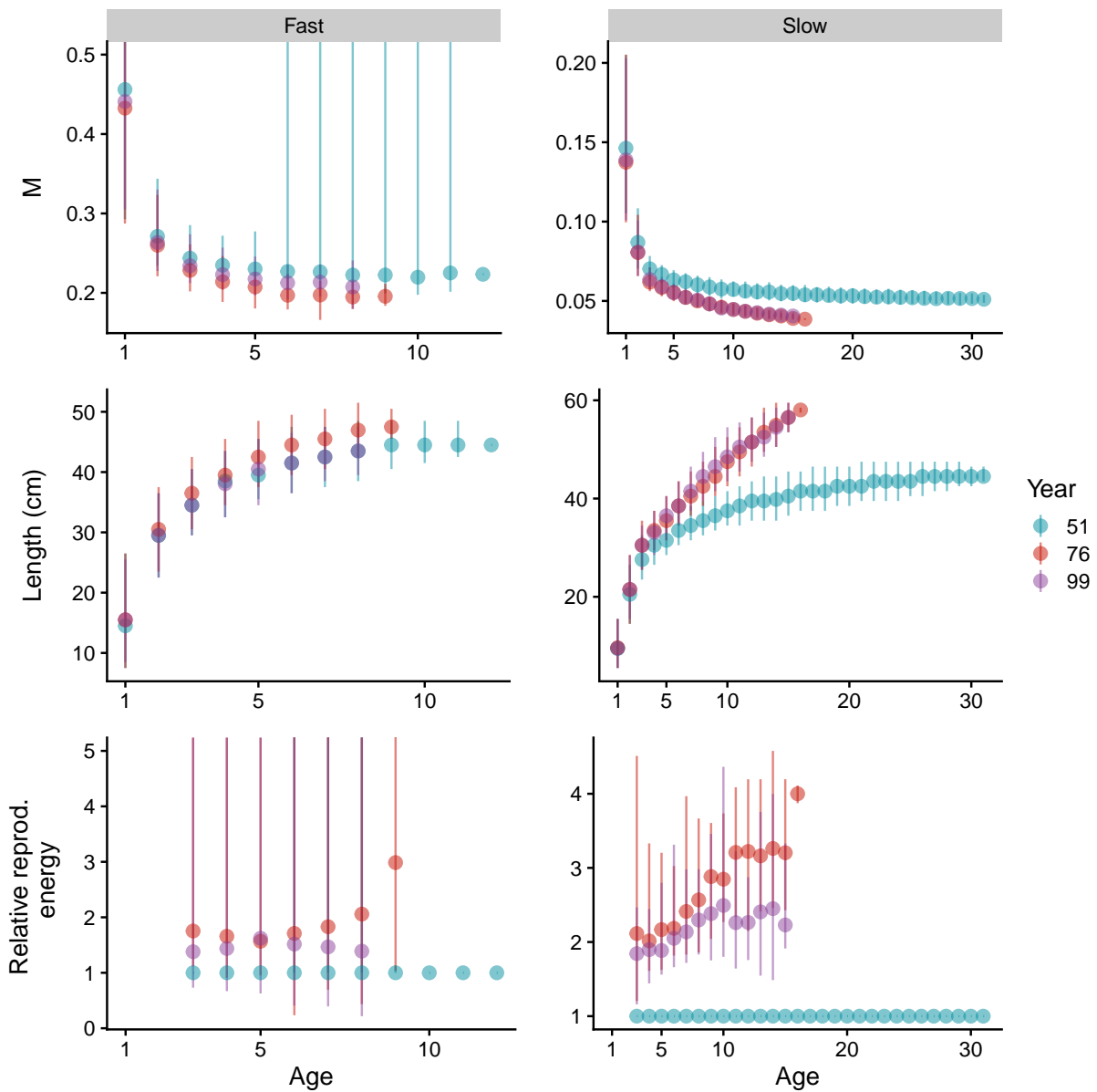


Figure 5: Simulated values for productivity parameters for a single replicate for the base environmental scenario (constant temperature, constant environment). All parameters are shown as abundance-at-size weighted means-at-age for fish stocks with fast (left column) and slow (right column) life histories at the beginning of fishing (year 51), halfway through the fishing history (year 76), and for the final fishing year (year 99). Parameters are: natural mortality (M), length-at-age (Length), and relative reproductive energy. The simulation applied constant fishing mortality.

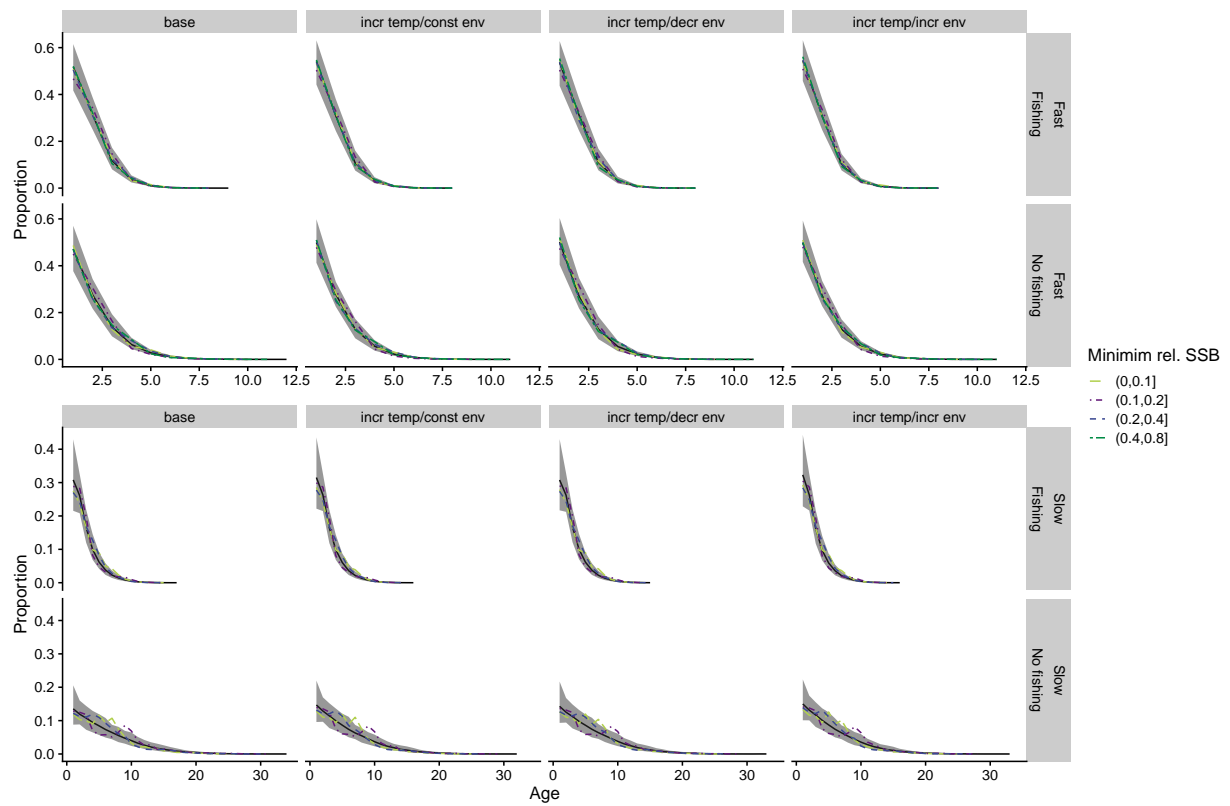


Figure 6: Trajectories of simulated proportions-at-age in the final fishing year for fish stocks with fast (top two rows) and slow (bottom two rows) life histories, with fishing mortality constant. Shown are the median by year (black line) and the 95% inter-quartile range of simulations (grey shaded area) with proportions-at-age across all simulations, and randomly selected simulation replicates across levels of minimum relative stock biomass (coloured and dashed lines). Simulations were with and without fishing for four different climate scenarios: base, no temperature or environmental change; incr temp/const env, increasing temperature, no environmental change; incr temp/decr env, increasing temperature, declining environment; incr temp/incre env, increasing temperature, increasing environmental suitability.

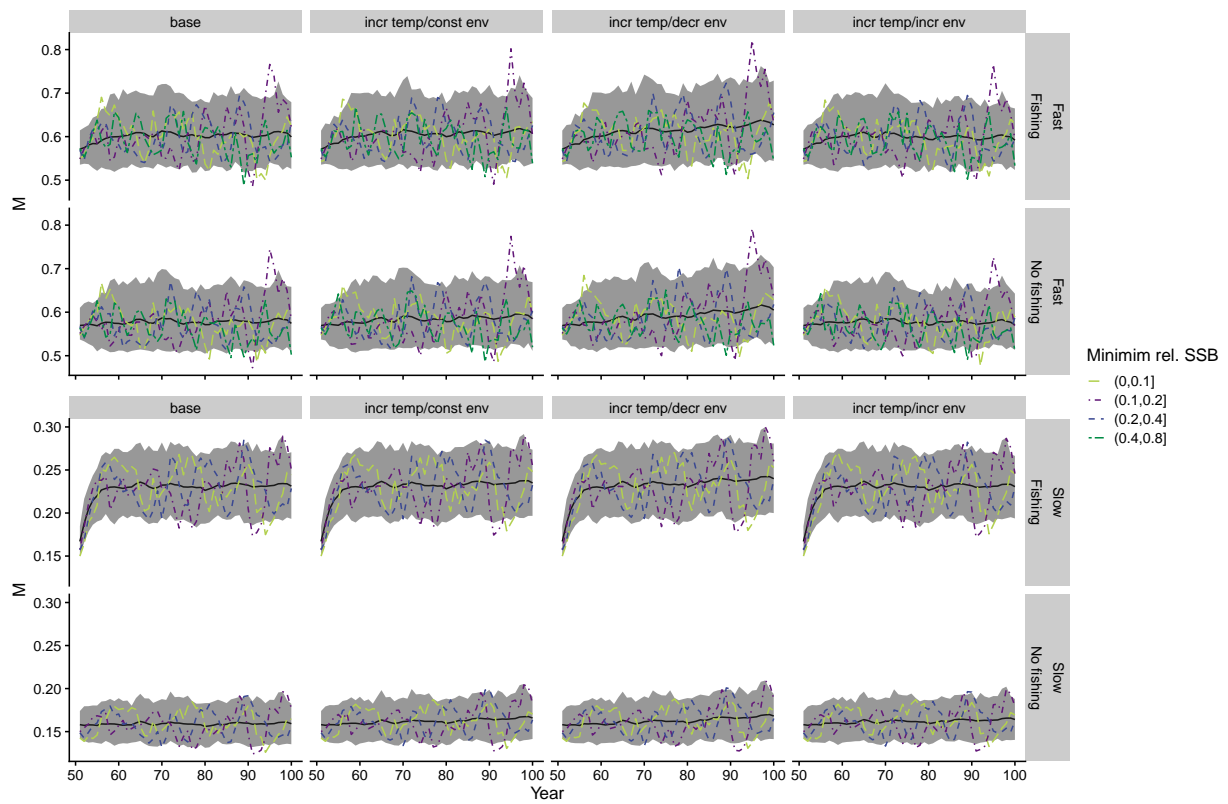


Figure 7: Trajectories of simulated natural mortality M (abundance-weighted mean natural mortality) for fish stocks with fast (top two rows) and slow (bottom two rows) life histories, with fishing mortality constant. Shown are the median by year (black line) and the 95% inter-quantile range of simulations (grey shaded area) with M across all simulations, and randomly selected simulation replicates across levels of minimum relative stock biomass (coloured and dashed lines). Simulations were with and without fishing for four different climate scenarios: base, no temperature or environmental change; incr temp/const env, increasing temperature, no environmental change; incr temp/decr env, increasing temperature, declining environment; incr temp/incr env, increasing temperature, increasing environmental suitability.

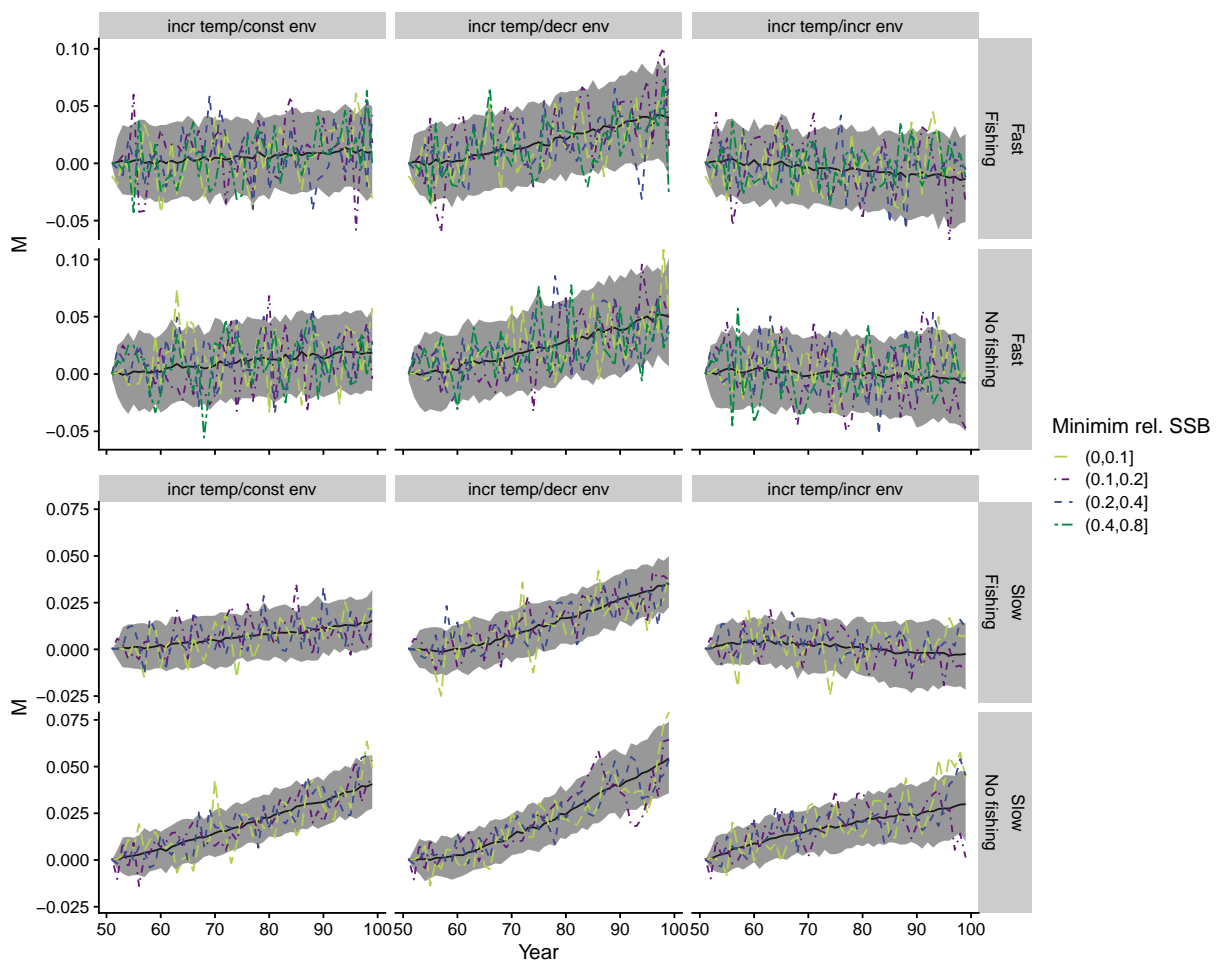


Figure 8: Trajectories of relative natural mortality M (abundance-weighted mean natural mortality) relative to the base scenario for fish stocks with fast (top two rows) and slow (bottom two rows) life histories, with fishing mortality constant. Shown are the median by year (black line) and the 95% inter-quantile range of simulations (grey shaded area) with M across all simulations, and randomly selected simulation replicates across levels of minimum relative stock biomass (coloured and dashed lines). Simulations were with and without fishing for three different climate scenarios, relative to the base scenario (no temperature or environmental change): incr temp/const env, increasing temperature, no environmental change; incr temp/decr env, increasing temperature, declining environment; incr temp/incre env, increasing temperature, increasing environmental suitability.

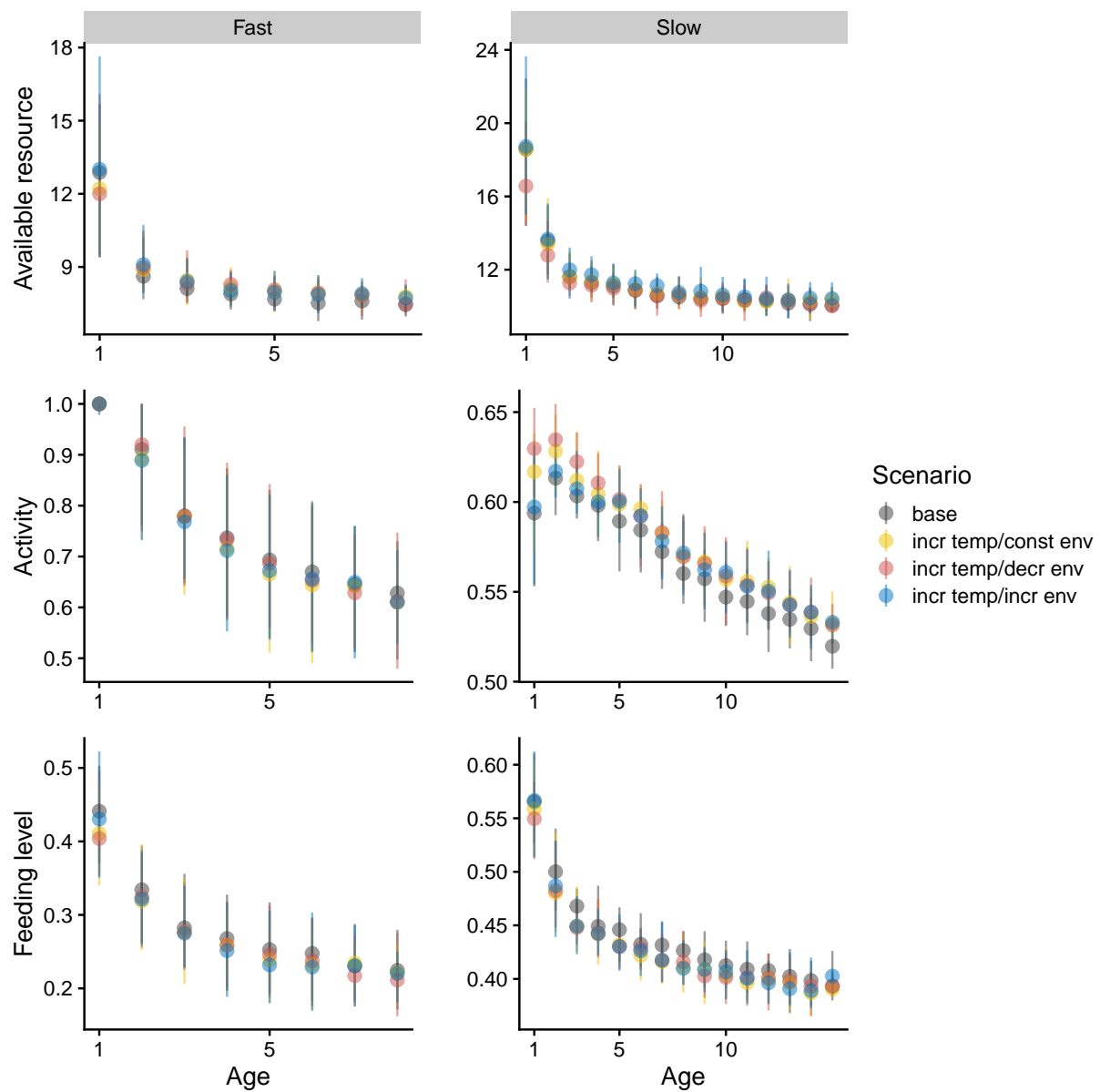


Figure 9: Simulated values for parameters related to feeding rates for a single replicate for four different climate scenarios: base, no temperature or environmental change; incr temp/const env, increasing temperature, no environmental change; incr temp/decr env, increasing temperature, declining environment; incr temp/incr env, increasing temperature, increasing environmental suitability. All parameters are shown as abundance-at-size weighted means-at-age for fish stocks with fast (left column) and slow (right column) life histories for the final fishing year (year 99). Parameters were: available resource (prey encounter rate $\gamma\Theta$), activity level, and feeding level (fraction of maximum consumption). The simulation applied constant fishing mortality.

Similar density-dependent increases in growth rates (von Bertalanffy K) initially appeared with decreasing stock size from fishing (see Figure 5); however, these increases reverted to previous growth rates over a relatively short time frame of about a decade (Figure 10). Climate trends led to increases in K , which were attenuated by declines in environmental suitability, but accentuated by increases in bottom-up productivity (Figure 11).

Although K appeared to revert to unfished parameter values, L_∞ increased with fishing alone due to density-dependent increase of per-capita resources (Figure 12). This trend was evident even for fast life-history species, for which most other parameters appeared to show little response to fishing. Contrary to K and M , the different climate scenarios all led to declines in L_∞ (Figure 13). These declines were accentuated for fished replicates relative to their unfished counterparts.

The aggregate spawning potential increased under fishing for both life histories, mirroring initial increases in K and L_∞ (Figure 14). The initial increase quickly levelled off, following the similar trajectory in K (see Figure 10). For stocks with a slow life history, this initial response was similar across nearly all simulation replicates. In contrast, for stocks with a fast life history, a more variable initial response was evident among replicates, depending on environmental signals during this period.

Compared with density-dependent responses to fishing and annual to decadal fluctuations in environmental suitability and temperature, mean productivity responses to gradual shifts in the environment were relatively small, but led to declines (Figure 15). Aggregate productivity changes were also slightly more pronounced for fished than for unfished replicates, despite opposing patterns in M and K (i.e., stronger response for unfished scenarios). All of the individual productivity parameters combined explained the changes in aggregate productivity; however, none were influential by themselves (Figure 16).

Constant catch simulations produced similar results, but there was considerably more variability both in individual parameter trends and in their response to climate-forcing simulations and fishing (see Appendix B, Figures B-1 to B-14 for constant catch simulations). In general, responses for fished populations were markedly more variable than for unfished populations, owing to changes in the density of fished stocks under variable fixed catches across replicates.

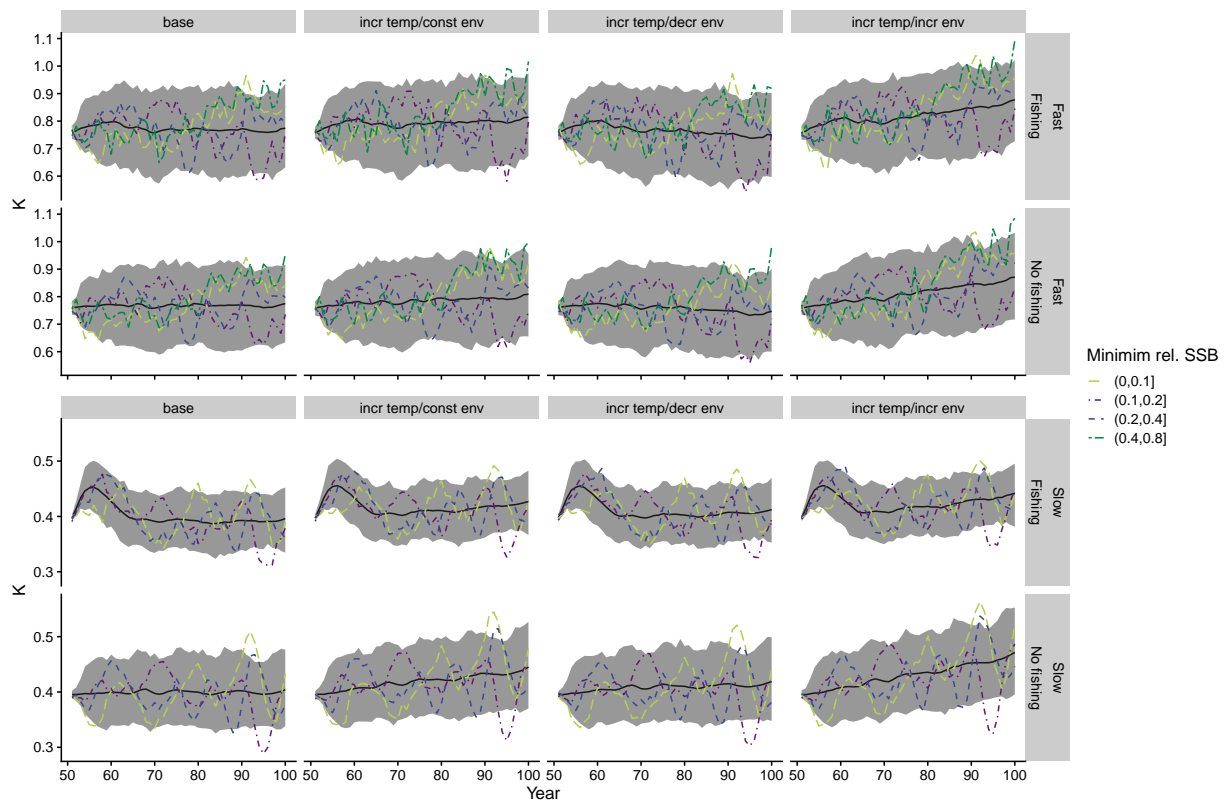


Figure 10: Trajectories of simulated von Bertalanffy growth rate K (estimated from length-at-age for each year) for fish stocks with fast (top two rows) and slow (bottom two rows) life histories across all simulations, with fishing mortality constant. Shown are the median by year (black line) and the 95% inter-quartile range of simulations (grey shaded area) with K across all simulations, and randomly selected simulation replicates across levels of minimum relative stock biomass (coloured and dashed lines). Simulations were with and without fishing for four different climate scenarios: base, no temperature or environmental change; incr temp/const env, increasing temperature, no environmental change; incr temp/decr env, increasing temperature, declining environment; incr temp/incre env, increasing temperature, increasing environmental suitability.

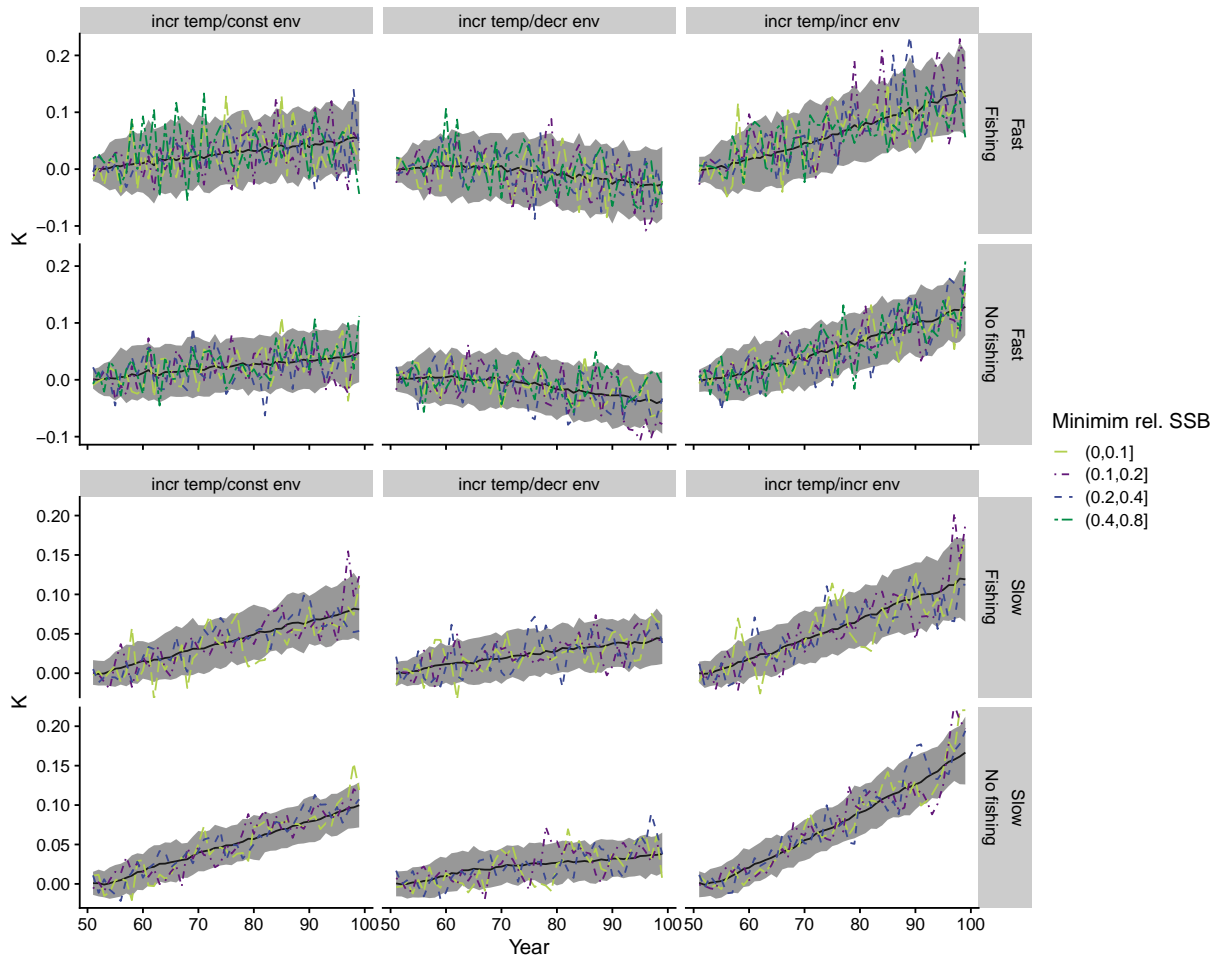


Figure 11: Trajectories of relative von Bertalanffy growth rate K (estimated from length-at-age for each year) relative to the base scenario for fish stocks with fast (top two rows) and slow (bottom two rows) life histories, with fishing mortality constant. Shown are the median by year (black line) and the 95% inter-quartile range of simulations (grey shaded area) with K across all simulations, and randomly selected simulation replicates across levels of minimum relative stock biomass (coloured and dashed lines). Simulations were with and without fishing for three different climate scenarios, relative to the base scenario (no temperature or environmental change): incr temp/const env, increasing temperature, no environmental change; incr temp/decr env, increasing temperature, declining environment; incr temp/incr env, increasing temperature, increasing environmental suitability.

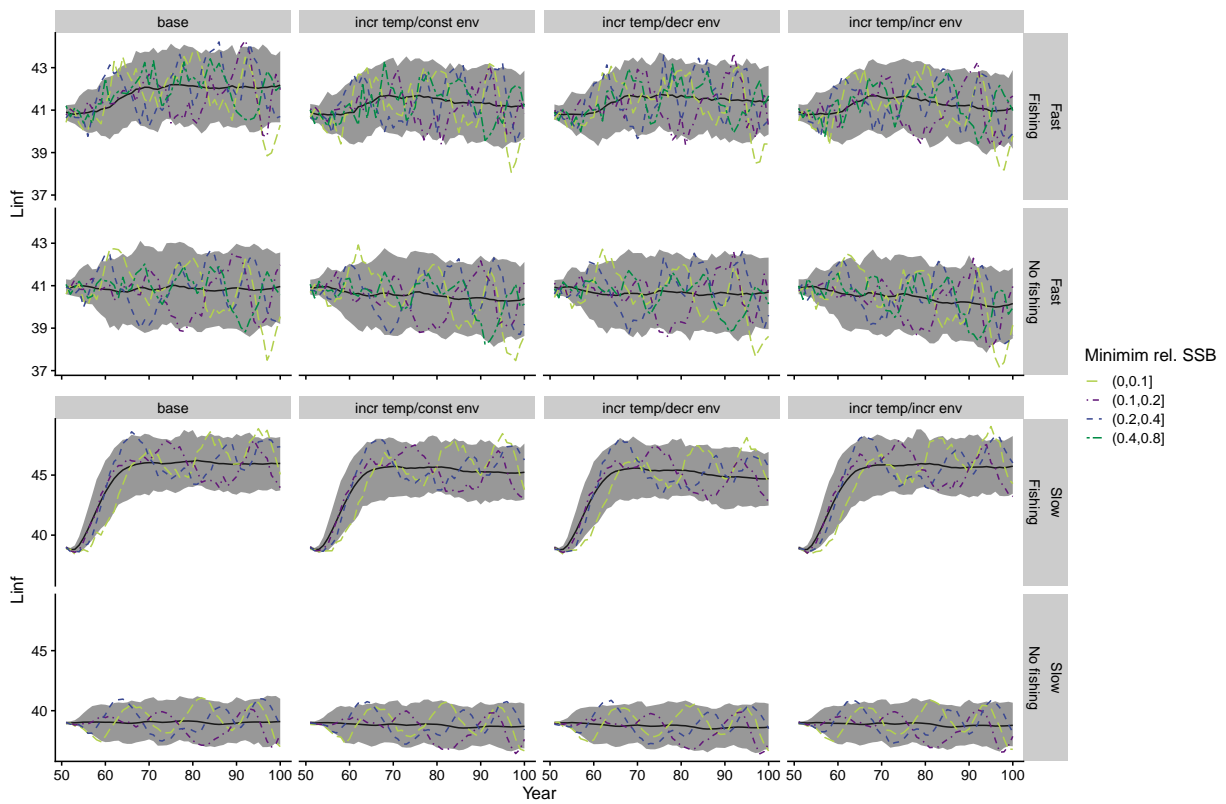


Figure 12: Trajectories of simulated asymptotic fish size L_∞ (estimated by fitting von Bertalanffy growth curves from length-at-age for each year) for fish stocks with fast (top two rows) and slow (bottom two rows) life histories, with fishing mortality constant. Shown are the median by year (black line) and the 95% inter-quantile range of simulations (grey shaded area) with L_∞ across all simulations, and randomly selected simulation replicates across levels of minimum relative stock biomass (coloured and dashed lines). Simulations were with and without fishing for four different climate scenarios: base, no temperature or environmental change; incr temp/const env, increasing temperature, no environmental change; incr temp/decr env, increasing temperature, declining environment; incr temp/incre env, increasing temperature, increasing environmental suitability.

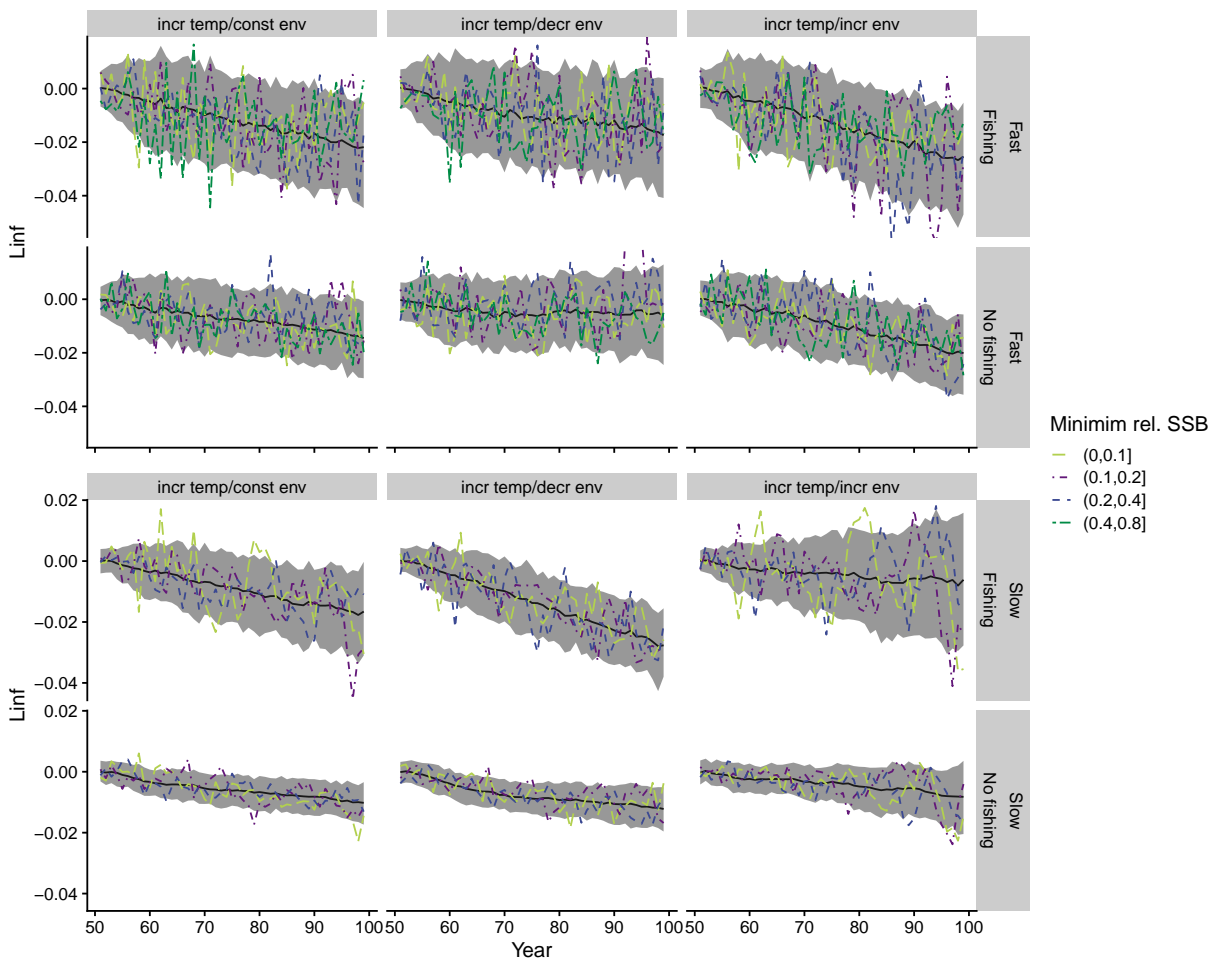


Figure 13: Trajectories of relative asymptotic fish size L_∞ (estimated by fitting von Bertalanffy growth curves from length-at-age for each year) relative to the base scenario for fish stocks with fast (top two rows) and slow (bottom two rows) life histories, with fishing mortality constant. Shown are the median by year (black line) and the 95% inter-quartile range of simulations (grey shaded area) with L_∞ across all simulations, and randomly selected simulation replicates across levels of minimum relative stock biomass (coloured and dashed lines). Simulations were with and without fishing for three different climate scenarios, relative to the base scenario (no temperature or environmental change): incr temp/const env, increasing temperature, no environmental change; incr temp/decr env, increasing temperature, declining environment; incr temp/incre env, increasing temperature, increasing environmental suitability.

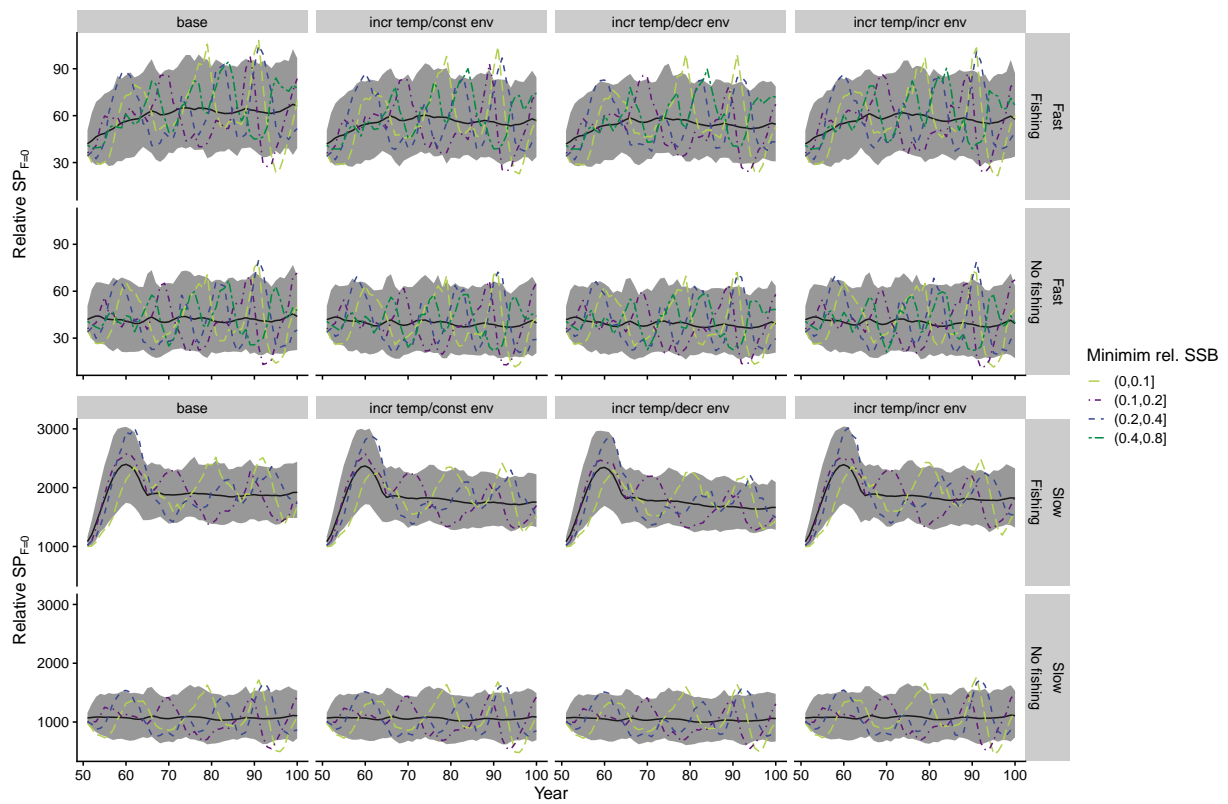


Figure 14: Trajectories of instantaneous spawning potential without fishing $SP_{F=0}$ (calculated taking annually-realised productivity parameter values across age classes present in that year) for fish stocks with fast (top two rows) and slow (bottom two rows) life histories, with fishing mortality constant. Shown are the median by year (black line) and the 95% inter-quartile range of simulations (grey shaded area) with $SP_{F=0}$ across all simulations, and randomly selected simulation replicates across levels of minimum relative stock biomass (coloured and dashed lines). Simulations were with and without fishing for four different climate scenarios: base, no temperature or environmental change; incr temp/const env, increasing temperature, no environmental change; incr temp/decr env, increasing temperature, declining environment; incr temp/incre env, increasing temperature, increasing environmental suitability.

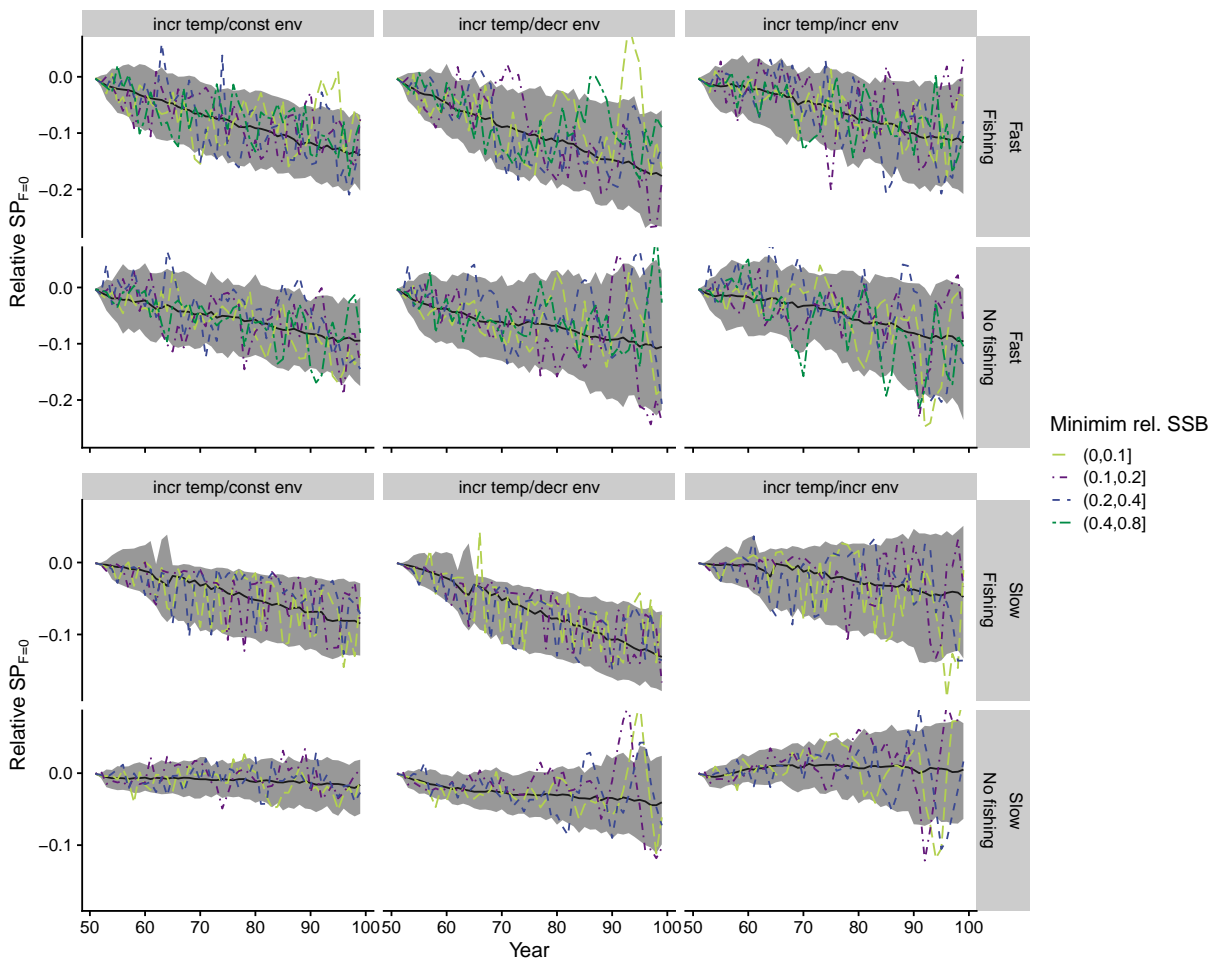


Figure 15: Trajectories of relative instantaneous spawning potential without fishing $SP_{F=0}$ (calculated taking annually-realised productivity parameter values across age classes present in that year) relative to the base scenario for fish stocks with fast (top two rows) and slow (bottom two rows) life histories, with fishing mortality constant. Shown are the median by year (black line) and the 95% inter-quartile range of simulations (grey shaded area) with $SP_{F=0}$ across all simulations, and randomly selected simulation replicates across levels of minimum relative stock biomass (coloured and dashed lines). Simulations were with and without fishing for three different climate scenarios, relative to the base scenario (no temperature or environmental change): incr temp/const env, increasing temperature, no environmental change; incr temp/decr env, increasing temperature, declining environment; incr temp/incre env, increasing temperature, increasing environmental suitability.

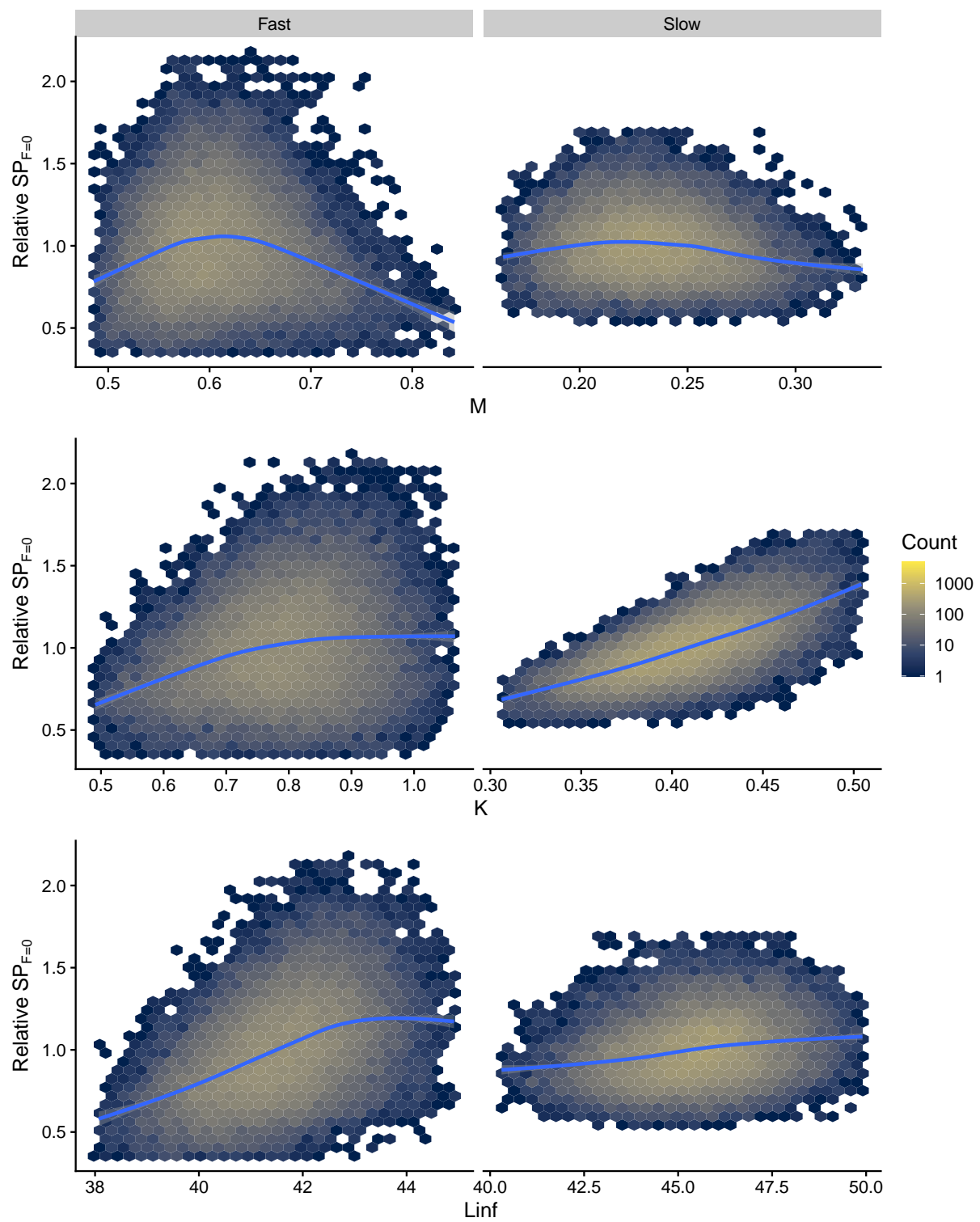


Figure 16: Correlation between spawning potential without fishing $SP_{F=0}$ (calculated taking annually-realised productivity parameter values across age classes present in that year) and individual productivity parameters in the model for simulations with constant fishing mortality for fish stocks with fast (left column) and slow (right column) life histories . Production parameters were: M , natural mortality; K , on Bertalanffy growth rate; L_{∞} (L_{inf}), asymptotic fish size.

4. DISCUSSION

This study aimed to build models that provide a starting point for integrating physiological, ecological, and fishery responses of fish stocks into a consistent framework. We focused on determinants and patterns of change in productivity parameters that are relevant to fisheries assessment and management. This focus was aimed at providing insights into the types of fish stock responses that can be expected in fluctuating environments, and also under long-term directional change relating to climate change.

The current modelling indicated responses in single productivity parameters that were consistent among simulation replicates: as expected, growth rate K , natural mortality M , and asymptotic fish size L_∞ all varied with temperature and environmental signals. Increases in K can be linked to the physiological basis for the model and the interpretation of K in terms of catabolism (metabolic cost K in the current simulations) in the von Bertalanffy growth model. In this context, the model performed similarly to a process-oriented version of the von Bertalanffy growth model. This aspect explains the predicted increases in K with temperature. Similarly, declines in L_∞ can be explained in terms of temperature dependence of K , if L_∞ is anabolism divided by catabolism.

Nevertheless, the framework of the von Bertalanffy growth model does not include a number of important concepts, precluding it from functioning as a basis for the exploration of different scenarios used here. For example, the energy balance in the von Bertalanffy growth model does not capture energy allocated to reproduction (Kozlowski et al. 2004, Quince et al. 2008), nor does it provide a coherent description of changes in consumption (anabolism). The model used in this study provided a mechanistic link between food resources, temperature, and physiological constraints: all else being equal, increased temperature led to increased foraging to offset metabolic requirements, with higher natural mortality M resulting from increased risk (Neubauer & Andersen 2019; and see Figure 9).

Although effects of temperature and the environment on isolated productivity parameters were predicted and explained by the current model, their aggregate effect on stock productivity was less obvious: even though growth rates increased with temperature, concomitant increases in M and declines in L_∞ led to an overall decline in productivity capacity. This decline occurred even though increases in K were more substantial (in relative terms) than changes in M and L_∞ . The relative magnitude of change in parameters relevant to productivity is, therefore, not necessarily an indication of the overall productivity trend. In stock assessments, often the most easily measured and detected changes are changes in growth rates, owing to their strong density-dependent and temperature-driven responses. Nevertheless, growth rates alone may give a false sense of temperature-driven productivity changes.

In natural systems, climate does not affect a single species in isolation, but determines changes in the ecosystem at all levels. These changes lead to concurrent effects on target stocks through their physiology and bottom-up or top-down determinants of productivity.

Although species have been shown to track temperature velocities across their ranges (Pinsky et al. 2013), in any particular point in space, productivity may increase or decrease; e.g., for stocks defined by geographical boundaries (Free et al. 2019). Nevertheless, globally, impacts associated with temperature have led to more declines than productivity increases. This trend was reflected in the current simulations, which suggest that temperature alone would negatively impact productivity of locally adapted species unless ecosystem changes are sufficient to counteract temperature impacts.

Temperature increases and ecosystem impacts were simulated here to be of similar magnitude for the different climate scenarios; however, this pattern is dependent on assumptions about the magnitude of bottom-up forcing in the model. The current study assumed only moderate directional trends in environmental suitability for climate scenarios, whereas temperature changes were assumed to be 5-fold compared with environmental forcing. The relative forcing was used partly for convenience—a marked decrease in mean habitat suitability in conjunction with interannual and decadal fluctuations led to increasing numbers of replicates where species went extinct, especially in the presence of fishing.

Although this number (i.e., the proportion of collapsed populations) could be used as a metric of the strength of bottom-up effects, the computational demand of repeating a sufficient number of replicates at varying degrees of environmental change prevent this approach. The present approach suggests that even moderate changes in environmental suitability are sufficient to offset changes determined by direct temperature impacts on focal species.

Direct temperature impacts may be attenuated by adaptive potential or plastic changes in physiological rates over time (Sandblom et al. 2016, Moffett et al. 2018, Glazier et al. 2020). At the same time, these impacts may also be stronger than were simulated here, if the “costs” of maintaining feeding levels increase. For example, the fitness cost of offsetting metabolic costs of temperature increase scales strongly with the metabolic and mortality costs of foraging (Neubauer & Andersen 2019). The current study assumed relatively low additional metabolic and mortality costs, so that temperature impacts on productivity may be substantially higher in some species. Findings here indicated a change of about 10% for a 1-degree change in ambient temperature over a period of 50 years. This change is within the range of most populations surveyed in a previous study (Free et al. 2019).

Patterns in productivity in response to changes in temperature and environmental suitability are not independent of fishing: density dependence and changes in size and age structure interact with and amplify or attenuate climate trends (see also Szwalski 2019). Across replicates, density-dependent responses, especially to initial reductions in biomass through fishing, are considerably larger than responses due to climate impacts simulated here. Although the difference in magnitude depends markedly on the amount of environmental forcing assumed, the current simulations showed that for stocks with marked fluctuations in abundance, density dependence can potentially mask or accentuate climate signals. In addition, truncation of age and size structure from fishing, in conjunction with removal of density-dependent constraints, is likely to lead to tighter coupling of stocks to environmental signals (Planque et al. 2010, Shelton & Mangel 2011). This aspect explains why productivity measured as spawning potential declined more markedly for fished than unfished stocks.

Overall, and in the context of New Zealand species, it is not possible to define a universal response of stock productivity to climate and environmental variability (see also Cummings et al. 2021, Dunn et al. 2022). Although changes for parameters like recruitment success, M and K may be predictable on the basis of temperature (Francis 1993, Parsons et al. 2021), and their trajectory and that of stock productivity as a whole (i.e., surplus production or spawning potential) depend on the evolution of all productivity parameters. Trends in measurable parameters such as K alone do, therefore, not necessarily provide adequate information on changes in productivity. In addition, mobile species will likely follow environmental gradients in habitat suitability (Dunn et al. 2022), either actively or via selection pressure and inter-generational shifts. For geographically constrained stock management boundaries, these changes could manifest in apparent declines or increases in biomass (i.e., sudden pulses in productivity) in these areas (Dunn et al. 2022). Nevertheless, given the potential for similar sudden pulses in low or high productivity within the closed populations simulated here, only large-scale analyses of coherent patterns could potentially distinguish local productivity changes from larger-scale immigration or emigration patterns determined by changing environments (e.g., Pinsky et al. 2013).

5. ACKNOWLEDGEMENTS

The authors thank Mary Livingston, Pamela Mace, and members of the Biodiversity Research Advisory Group and the Statistics, Assessment and Methods Working Group for comments and suggestions over the course of this project. The project was funded under Fisheries New Zealand project ZBD2018-03.

6. REFERENCES

- Andersen, K.H.; Beyer, J.E. (2006). Asymptotic size determines species abundance in the marine size spectrum. *The American Naturalist* 168 (1): 54–61.
- Andersen, K.H.; Beyer, J.E. (2013). Size structure, not metabolic scaling rules, determines fisheries reference points. *Fish and Fisheries* 16 (1): 1–22.
- Andersen, K.H.; Farnsworth, K.D.; Pedersen, M.; Gislason, H.; Beyer, J.E. (2009). How community ecology links natural mortality, growth, and production of fish populations. *ICES Journal of Marine Science: Journal du Conseil* 66 (9): 1978–1984. <https://doi.org/10.1093/icesjms/fsp061>
- Andersen, K.H.; Jacobsen, N.S.; Jansen, T.; Beyer, J.E. (2017). When in life does density dependence occur in fish populations? *Fish and Fisheries* 18 (4): 656–667.
- Brander, K.; Neuheimer, A.; Andersen, K.H.; Hartvig, M. (2013). Overconfidence in model projections. *ICES Journal of Marine Science* 70 (6): 1065–1068. <https://doi.org/10.1093/icesjms/fst055>
- Brander, K.M. (2007). Global fish production and climate change. *Proceedings of the National Academy of Sciences* 104 (50): 19709–19714.
- Brett, J. (1965). The relation of size to rate of oxygen consumption and sustained swimming speed of sockeye salmon (*Oncorhynchus nerka*). *Journal of the Fisheries Board of Canada* 22 (6): 1491–1501.
- Britten, G.L.; Dowd, M.; Worm, B. (2016). Changing recruitment capacity in global fish stocks. *Proceedings of the National Academy of Sciences* 113 (1): 134–139. <https://doi.org/10.1073/pnas.1504709112>
- Charnov, E.L.; Gislason, H.; Pope, J.G. (2013). Evolutionary assembly rules for fish life histories. *Fish and Fisheries* 14 (2): 213–224. <https://doi.org/10.1111/j.1467-2979.2012.00467.x>
- Cummings, V.J.; Lundquist, C.J.; Dunn, M.R.; Francis, M.; Horn, P.L.; Law, C.; Pinkerton, M.H.; Sutton, P.; Tracey, D.M.; Hansen, L.J. (2021). Assessment of potential effects of climate-related changes in coastal and offshore waters on New Zealand's seafood sector. *New Zealand Aquatic Environment and Biodiversity Report* 261. 153 p.
- Deutsch, C.; Ferrel, A.; Seibel, B.; Pörtner, H.-O.; Huey, R.B. (2015). Climate change tightens a metabolic constraint on marine habitats. *Science* 348 (6239): 1132–1135. <https://doi.org/10.1126/science.aaa1605>
- Dunn, M.R.; Goeden, Z.; Neubauer, P.; Behrens, E.; Arnold, R. (2022). Climate change and the distribution of commercially caught marine fish species in New Zealand. Part 2: Predicting changes in distribution. *New Zealand Aquatic Environment and Biodiversity Report* 287. 155 p.
- Francis, M.P. (1993). Does water temperature determine year class strength in New Zealand snapper (*Pagrus auratus*, Sparidae)? *Fisheries Oceanography* 2 (2): 65–72. <https://doi.org/10.1111/j.1365-2419.1993.tb00121.x>
- Free, C.M.; Thorson, J.T.; Pinsky, M.L.; Oken, K.L.; Wiedenmann, J.; Jensen, O.P. (2019). Impacts of historical warming on marine fisheries production. *Science* 363 (6430): 979–983.
- Gilliam, J.F.; Fraser, D.F. (1987). Habitat selection under predation hazard: Test of a model with foraging minnows. *Ecology* 68 (6): 1856–1862.
- Gillooly, J.F.; Brown, J.H.; West, G.B.; Savage, V.M.; Charnov, E.L. (2001). Effects of size and temperature on metabolic rate. *Science* 293 (5538): 2248–2251.
- Glazier, D.S. (2009). Activity affects intraspecific body-size scaling of metabolic rate in ectothermic animals. *Journal of Comparative Physiology B* 179 (7): 821–828. <https://doi.org/10.1007/s00360-009-0363-3>
- Glazier, D.S.; Gring, J.P.; Holsopple, J.R.; Gjoni, V. (2020). Temperature effects on metabolic scaling of a keystone freshwater crustacean depend on fish-predation regime. *Journal of Experimental Biology* 223 (21).
- Gnauck, A.; Straškraba, M. (2013). *Freshwater ecosystems: Modelling and simulation* (Vol. 8). Elsevier.
- Hartvig, M.; Andersen, K.H.; Beyer, J.E. (2011). Food web framework for size-structured populations. *Journal of Theoretical Biology* 272 (1): 113–122.
- Holt, R.E.; Jorgensen, C. (2014). Climate warming causes life-history evolution in a model for Atlantic cod (*Gadus morhua*). *Conservation Physiology* 2 (1). <https://doi.org/10.1093/conphys/cou050>

- Holt, R.E.; Jorgensen, C. (2015). Climate change in fish: Effects of respiratory constraints on optimal life history and behaviour. *Biology Letters* 11 (2): 20141032–20141032. <https://doi.org/10.1098/rsbl.2014.1032>
- Jeschke, J.M.; Kopp, M.; Tollrian, R. (2002). Predator functional responses: Discriminating between handling and digesting prey. *Ecological Monographs* 72 (1): 95–112.
- Jutfelt, F.; Norin, T.; Ern, R.; Overgaard, J.; Wang, T.; McKenzie, D.J.; Lefevre, S.; Nilsson, G.E.; Metcalfe, N.B.; Hickey, A.J. (2018). Oxygen-and capacity-limited thermal tolerance: Blurring ecology and physiology. *Journal of Experimental Biology* 221 (1): jeb169615.
- Killen, S.S.; Atkinson, D.; Glazier, D.S. (2010). The intraspecific scaling of metabolic rate with body mass in fishes depends on lifestyle and temperature. *Ecology Letters* 13 (2): 184–193. <https://doi.org/10.1111/j.1461-0248.2009.01415.x>
- Kindsvater, H.K.; Mangel, M.; Reynolds, J.D.; Dulvy, N.K. (2016). Ten principles from evolutionary ecology essential for effective marine conservation. *Ecology and Evolution* 6 (7): 2125–2138.
- Kozlowski, J.; Czarnoleski, M.; Danko, M. (2004). Can optimal resource allocation models explain why ectotherms grow larger in cold? *Integrative and Comparative Biology* 44 (6): 480–493.
- Lefevre, S. (2016). Are global warming and ocean acidification conspiring against marine ectotherms? A meta-analysis of the respiratory effects of elevated temperature, high CO₂ and their interaction. *Conservation Physiology* 4 (1). <https://doi.org/10.1093/conphys/cow009>
- Lefevre, S.; McKenzie, D.J.; Nilsson, G.E. (2018). In modelling effects of global warming, invalid assumptions lead to unrealistic projections. *Global change biology* 24 (2): 553–556.
- Lefrancois, C.; Claireaux, G. (2003). Influence of ambient oxygenation and temperature on metabolic scope and scope for heart rate in the common sole *solea solea*. *Marine Ecology Progress Series* 259: 273–284.
- Mangel, M.; Brodziak, J.; DiNardo, G. (2010). Reproductive ecology and scientific inference of steepness: A fundamental metric of population dynamics and strategic fisheries management. *Fish and Fisheries* 11 (1): 89–104.
- Mangel, M.; MacCall, A.D.; Brodziak, J.; Dick, E.; Forrest, R.E.; Pourzand, R.; Ralston, S. (2013). A perspective on steepness, reference points, and stock assessment. *Canadian Journal of Fisheries and Aquatic Sciences* 70 (6): 930–940.
- Moffett, E.R.; Fryxell, D.C.; Palkovacs, E.P.; Kinnison, M.T.; Simon, K.S. (2018). Local adaptation reduces the metabolic cost of environmental warming. *Ecology* 99 (10): 2318–2326.
- Moore, J.K.; Fu, W.; Primeau, F.; Britten, G.L.; Lindsay, K.; Long, M.; Doney, S.C.; Mahowald, N.; Hoffman, F.; Randerson, J.T. (2018). Sustained climate warming drives declining marine biological productivity. *Science* 359 (6380): 1139–1143.
- Neubauer, P.; Andersen, K.H. (2019). Thermal performance of fish is explained by an interplay between physiology, behaviour, and ecology. *Conservation Physiology* 7: 1–14.
- Neubauer, P.; D’Amar, T.; Dunn, M. (2023). Climate impacts on fished populations. Part 2: Effects of climate and environmental variability on fishery stock assessment accuracy. *New Zealand Fisheries Assessment Report* 2023/57. 40 p.
- Parsons, D.M.; Allan, B.J.M.; Bian, R.; Herbert, N.A.; Gublin, Y.; McKenzie, J.R.; McMahon, S.; McQueen, D.; Pan, H.; Pether, S.; Radford, C.; Setiawan, A.; Munday, P. (2021). Ocean acidification and elevated temperature effects on new zealand snapper. *New Zealand Aquatic Environment and Biodiversity Report* 275. 58 p.
- Perry, R.I.; Cury, P.; Brander, K.; Jennings, S.; Möllmann, C.; Planque, B. (2010). Sensitivity of marine systems to climate and fishing: Concepts, issues and management responses. *Journal of Marine Systems* 79 (3-4): 427–435.
- Pinsky, M.L.; Worm, B.; Fogarty, M.J.; Sarmiento, J.L.; Levin, S.A. (2013). Marine taxa track local climate velocities. *Science* 341 (6151): 1239–1242. <https://doi.org/10.1126/science.1239352>
- Planque, B.; Fromentin, J.-M.; Cury, P.; Drinkwater, K.F.; Jennings, S.; Perry, R.I.; Kifani, S. (2010). How does fishing alter marine populations and ecosystems sensitivity to climate? *Journal of Marine Systems* 79 (3-4): 403–417.
- Priede, I.G. (1985). Metabolic scope in fishes. In: Fish energetics (pp. 33–64). Springer. Retrieved 2016-09-09, from <http://link.springer.com/chapter/10.1007/978-94-011-7918-82>

- Quince, C.; Abrams, P.A.; Shuter, B.J.; Lester, N.P. (2008). Biphasic growth in fish I: Theoretical foundations. *Journal of Theoretical Biology* 254 (2): 197–206. <https://doi.org/10.1016/j.jtbi.2008.05.029>
- Sainmont, J.; Andersen, K.H.; Thygesen, U.H.; Fiksen, Ø.; Visser, A.W. (2015). An effective algorithm for approximating adaptive behavior in seasonal environments. *Ecological Modelling* 311: 20–30. <https://doi.org/10.1016/j.ecolmodel.2015.04.016>
- Sandblom, E.; Clark, T.D.; Gräns, A.; Ekström, A.; Brijs, J.; Sundström, L.F.; Odelström, A.; Adill, A.; Aho, T.; Jutfelt, F. (2016). Physiological constraints to climate warming in fish follow principles of plastic floors and concrete ceilings. *Nature communications* 7 (1): 1–8.
- Sentis, A.; Hemptonne, J.-L.; Brodeur, J. (2013). Parsing handling time into its components: Implications for responses to a temperature gradient. *Ecology* 94 (8): 1675–1680. <https://doi.org/10.1890/12-2107.1>
- Shelton, A.O.; Mangel, M. (2011). Fluctuations of Fish Populations and the Magnifying Effects of Fishing. *Proceedings of the National Academy of Sciences* 108 (17): 7075–7080. <https://doi.org/10.1073/pnas.1100334108>
- Stock, C.A.; John, J.G.; Rykaczewski, R.R.; Asch, R.G.; Cheung, W.W.; Dunne, J.P.; Friedland, K.D.; Lam, V.W.; Sarmiento, J.L.; Watson, R.A. (2017). Reconciling fisheries catch and ocean productivity. *Proceedings of the National Academy of Sciences* 114 (8): E1441–E1449.
- Szuwalski, C. (2019). Comment on “impacts of historical warming on marine fisheries production”. *Science* 365 (6454): eaax5721.
- Szuwalski, C. (2016). Changing fisheries productivity and food security. *Proceedings of the National Academy of Sciences* 113 (13): E1773–E1774. <https://doi.org/10.1073/pnas.1600641113>
- Verberk, W.C.; Bilton, D.T.; Calosi, P.; Spicer, J.I. (2011). Oxygen supply in aquatic ectotherms: Partial pressure and solubility together explain biodiversity and size patterns. *Ecology* 92 (8): 1565–1572. <http://www.esajournals.org/doi/abs/10.1890/10-2369.1>

APPENDIX A: OXYGEN BUDGET

The oxygen budget $P_{O_2}(w, T)$ (or aerobic scope) follows a similar form to the mass budget:

$$P_{O_2}(w, T, \tau) = S_{O_2}(w, T) - D_{O_2}(w, T, \tau) \quad (\text{A-1})$$

$$= S_{O_2}(T)w^n - \omega c(T) (\beta f(w, T, \tau)hw^q + k_s w^n + k_a w). \quad (\text{A-2})$$

Demand ($D_{O_2}(w, T, \tau)$) is the sum of oxygen used for all metabolic processes in Equation 1 (except assimilation losses), and ω is the amount of oxygen required per mass. The oxygen supply ($S_{O_2}(w, T)$) scales with body weight as w^n multiplied by a flexible dome-shaped function that can emulate both a dome-shaped maximum oxygen supply (MOS) and a MOS that increases continuously up to a lethal temperature (Figure A-1).

The maximum oxygen consumption is the oxygen consumption during maximal activity level that can be sustained over some time, and corresponded to the maximum metabolic rate (MMR) in the current model. Although the MMR is often used synonymously with both MOS and demand, in some species, the maximal oxygen consumption ($D_{O_2}^{\max}(T)$) is not reached at maximum activity levels, but during digestion (Priede 1985).

In the present model, MMR and maximum oxygen supply were equivalent because contributions from anaerobic metabolism were not explicitly modelled, such as during burst swimming or hypoxia. During these events, the metabolic rate may be higher than oxygen consumption alone would suggest; however, these states cannot usually be sustained (and, therefore, were outside of the sustained MMR defined here)(see values of the oxygen supply in Table A-1).

This study assumed that oxygen supply, taken as the aggregated process of oxygen delivery from diffusion across respiratory organ membranes (e.g., gills) to delivery for cellular metabolism, is temperature-dependent and follows a flexible dome-shaped function (Lefrancois & Claireaux 2003, Gnauck & Straškraba 2013):

$$S_{O_2}(T) = \lambda(T) \left(1 - e^{(C_{O_2}(T) - C_{O_2}^{\text{crit}}) \log(0.5) / (C_{O_2}^{50} - C_{O_2}^{\text{crit}})} \right), \quad (\text{A-3})$$

$$\lambda(T) = \zeta \left(\frac{T_{\max} - T}{T_{\max} - T_{\text{opt}}} \right)^{\eta} \times \exp \left(-\eta \frac{T_{\max} - T}{T_{\max} - T_{\text{opt}}} \right). \quad (\text{A-4})$$

Here, $\lambda(T)$ specifies the temperature dependency of O_2 supply, whereas the second term in $S_{O_2}(T)$ term describes the dependence on ambient O_2 concentrations at temperature T ($C_{O_2}(T)$). At constant temperature T , oxygen supply is a function of ambient oxygen and is assumed to follow a saturating function (e.g., Lefrancois & Claireaux 2003). We specified $C_{O_2}^{50}$ as the point where oxygen supply has dropped by 50% relative to the saturation level $\lambda(T)$, and $C_{O_2}^{\text{crit}}$ is the ambient concentration at which oxygen supply ceases (see the oxygen budget for both life histories in Table A-1).

Ambient oxygen concentration levels were assumed to decline with temperature according to a curve that approximates declines of dissolved oxygen in saltwater at 35 PSU (Practical Salinity Unit) as $l \cdot e^{-0.01851*(T-5)}$, with l the oxygen concentration at 5°C. To specify $\lambda(T)$, T_{\max} was defined as the lethal temperature for the species, and T_{opt} as the temperature at which oxygen supply is maximised; η determines the width of the dome-shape, and ζ its height. (Note that the simulated increase in the aggregated oxygen supply includes potential increases in oxygen delivery via increased diffusive (passive) supply at higher temperatures (Verberk et al. 2011); it also includes increased active delivery of oxygen

made possible by increased heart rates at higher temperatures (e.g., Lefrancois & Claireaux 2003). With the above formulation, an oxygen supply (and hence MMR) was emulated that increases up to the lethal temperature by setting the temperature for maximum oxygen delivery close to the lethal temperature (Figure A-1).

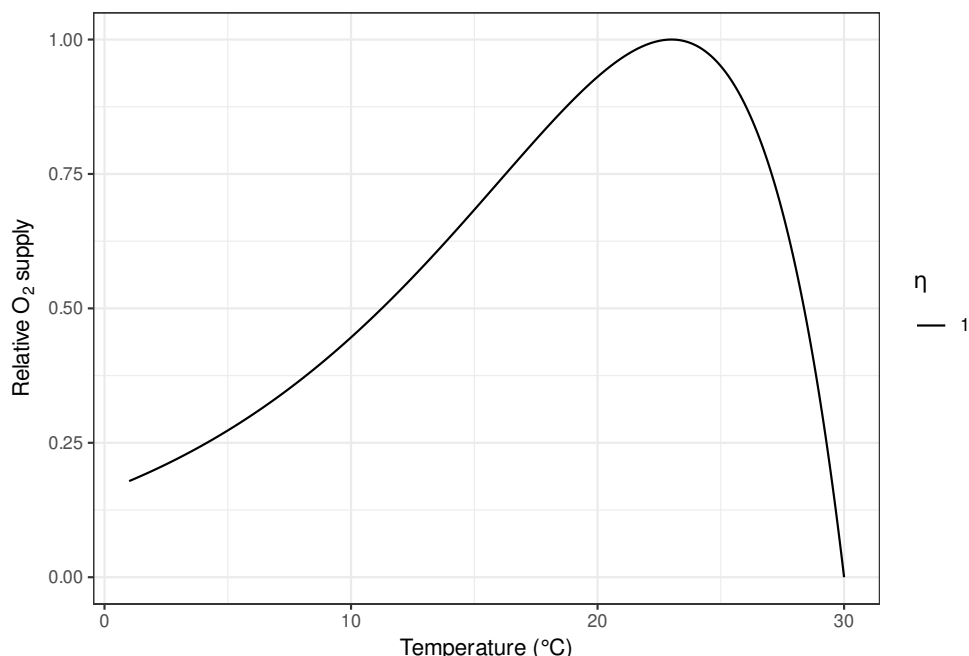


Figure A-1: Maximum oxygen supply (MOS) relative to the maximum supply for species with a dome-shaped MOS (here $\eta=3$) and a continually increasing MOS ($\eta=0.1$) used in the model scenarios.

Table A-1: Parameter definitions and values of the oxygen (O_2) budget for two species traits: slow and fast life histories or strategies.

Description	Symbol (unit)	Value	
		Slow strategy	Fast strategy
Critical O_2	$P_{\text{crit}} (\text{mg}\cdot\text{L}^{-1})$		2
Dissolved O_2 at $0.5 \times f_{\max}(O_2)$	$P_{50} (\text{mg}\cdot\text{L}^{-1})$		4
Doming for O_2 supply	η		1
Level of O_2 supply	$\zeta (\text{g}\cdot\text{y}^{-1})$	0.5	1

APPENDIX B: RESULTS FOR CONSTANT CATCH SIMULATIONS

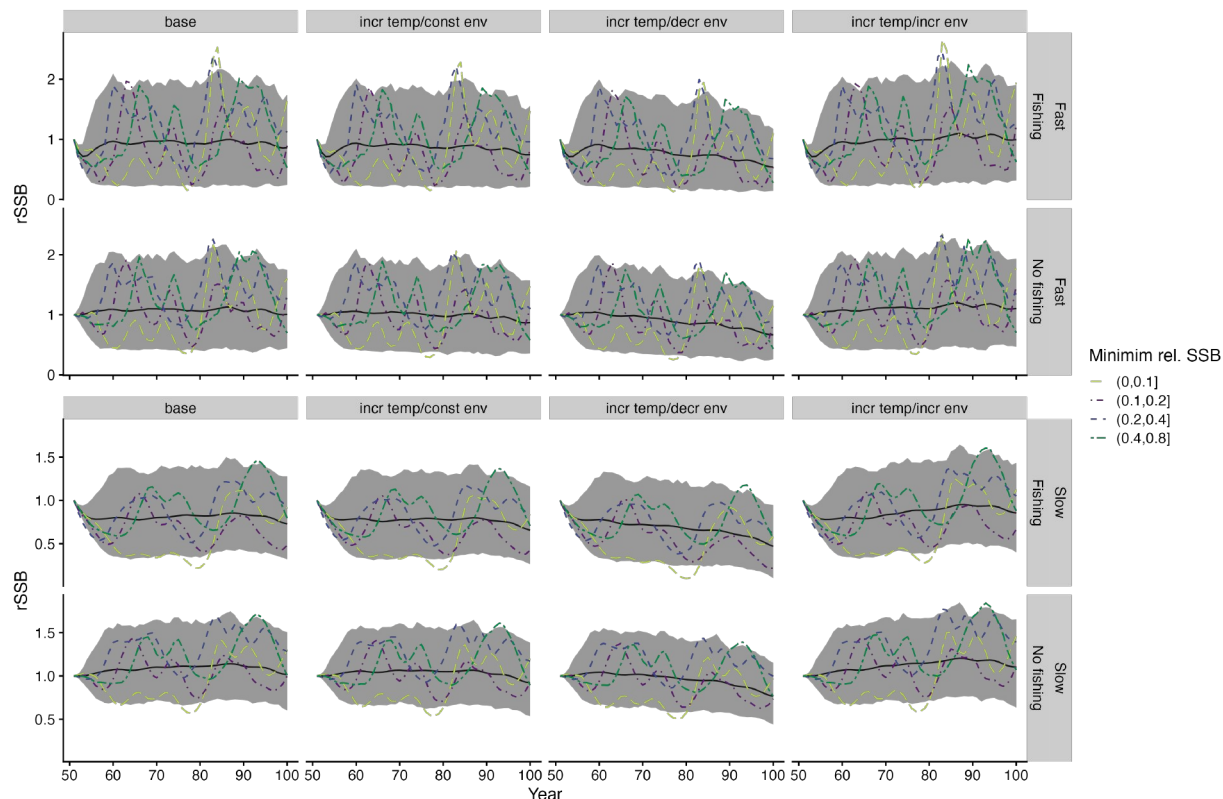


Figure B-1: Trajectories of simulated relative spawning stock biomass (rSSB) for fish stocks with fast (top two rows) and slow (bottom two rows) life histories, with catch constant. Shown are the median by year (black line) and the 95% inter-quantile range of simulations (grey shaded area) with rSSB across all simulations, and randomly selected simulation replicates (coloured and dashed lines). Simulations were with and without fishing for four different climate scenarios: base, no temperature or environmental change; incr temp/const env, increasing temperature, no environmental change; incr temp/decr env, increasing temperature, declining environment; incr temp/incre env, increasing temperature, increasing environmental suitability.

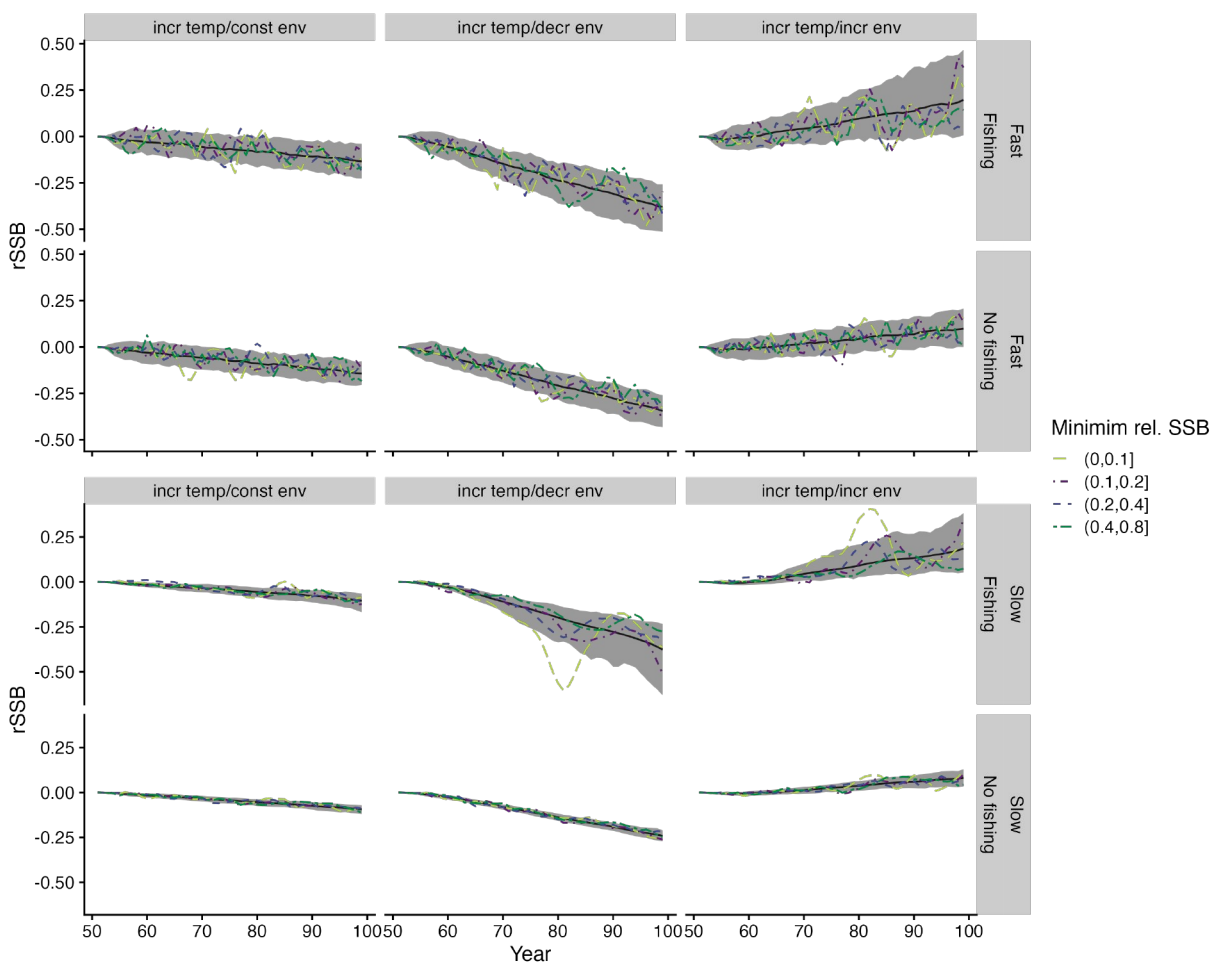


Figure B-2: Trajectories of simulated relative spawning stock biomass (rSSB) relative to the base scenario for fish stocks with fast (top two rows) and slow (bottom two rows) life histories, with catch constant. Shown are the median by year (black line) and the 95% inter-quantile range of simulations (grey shaded area) with rSSB across all simulations, and randomly selected simulation replicates (coloured and dashed lines). Simulations were with and without fishing for three different climate scenarios, relative to the base scenario (no temperature or environmental change): incr temp/const env, increasing temperature, no environmental change; incr temp/decr env, increasing temperature, declining environment; incr temp/incre env, increasing temperature, increasing environmental suitability.

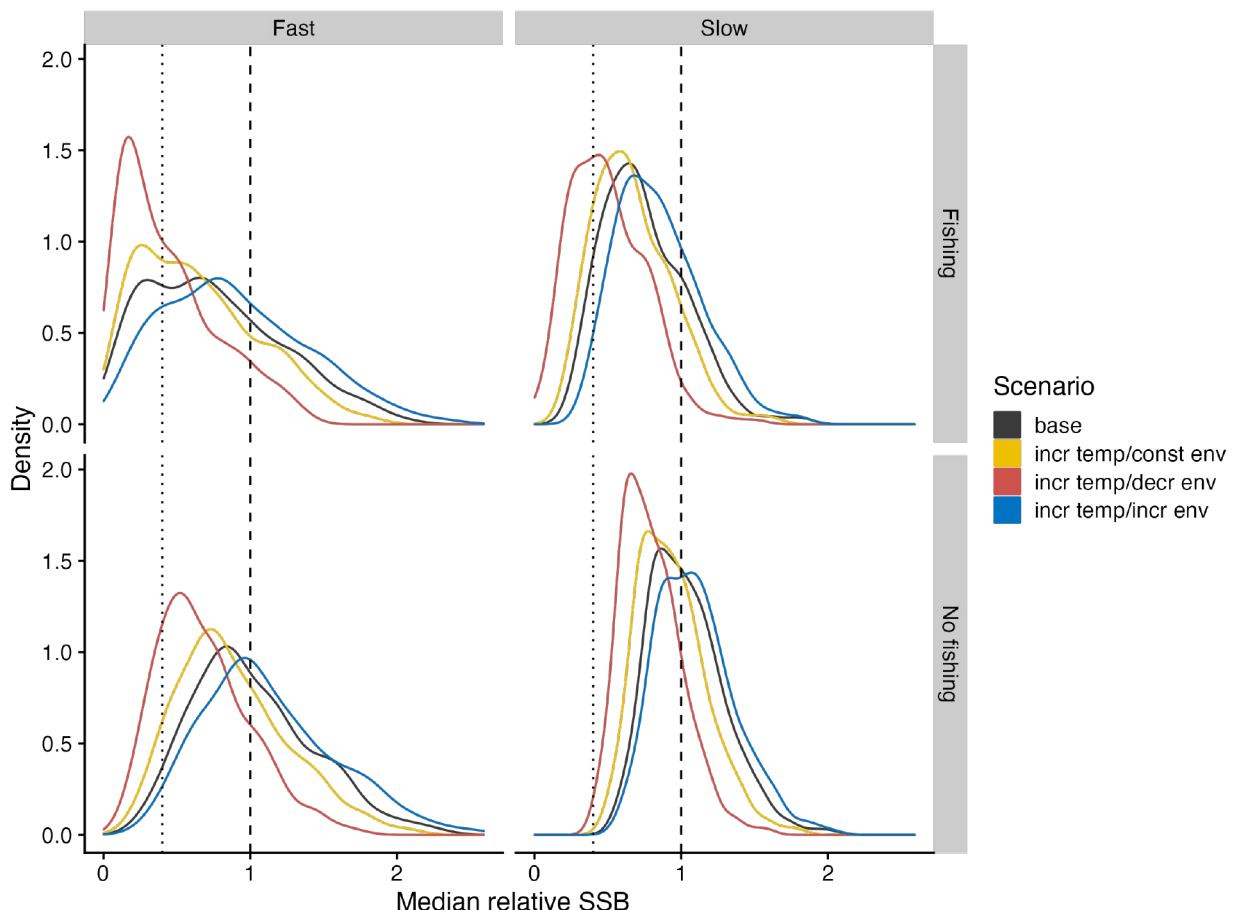


Figure B-3: Simulation outcomes for stock status (relative spawning stock biomass, rSSB) for the last simulation year of the current study for fish stocks with fast (left column) and slow (right column) life histories. Catch was assumed to be constant. Simulations were with and without fishing for four different climate scenarios: base, no temperature or environmental change; incr temp/const env, increasing temperature, no environmental change; incr temp/decr env, increasing temperature, declining environment; incr temp/incre env, increasing temperature, increasing environmental suitability. All simulation replicates started from the same random seed. Dotted line indicates $0.4 \cdot SSB_0$, dashed line SSB_0 , the spawning stock biomass at year 50 (i.e., before fishing commenced for fished scenarios).

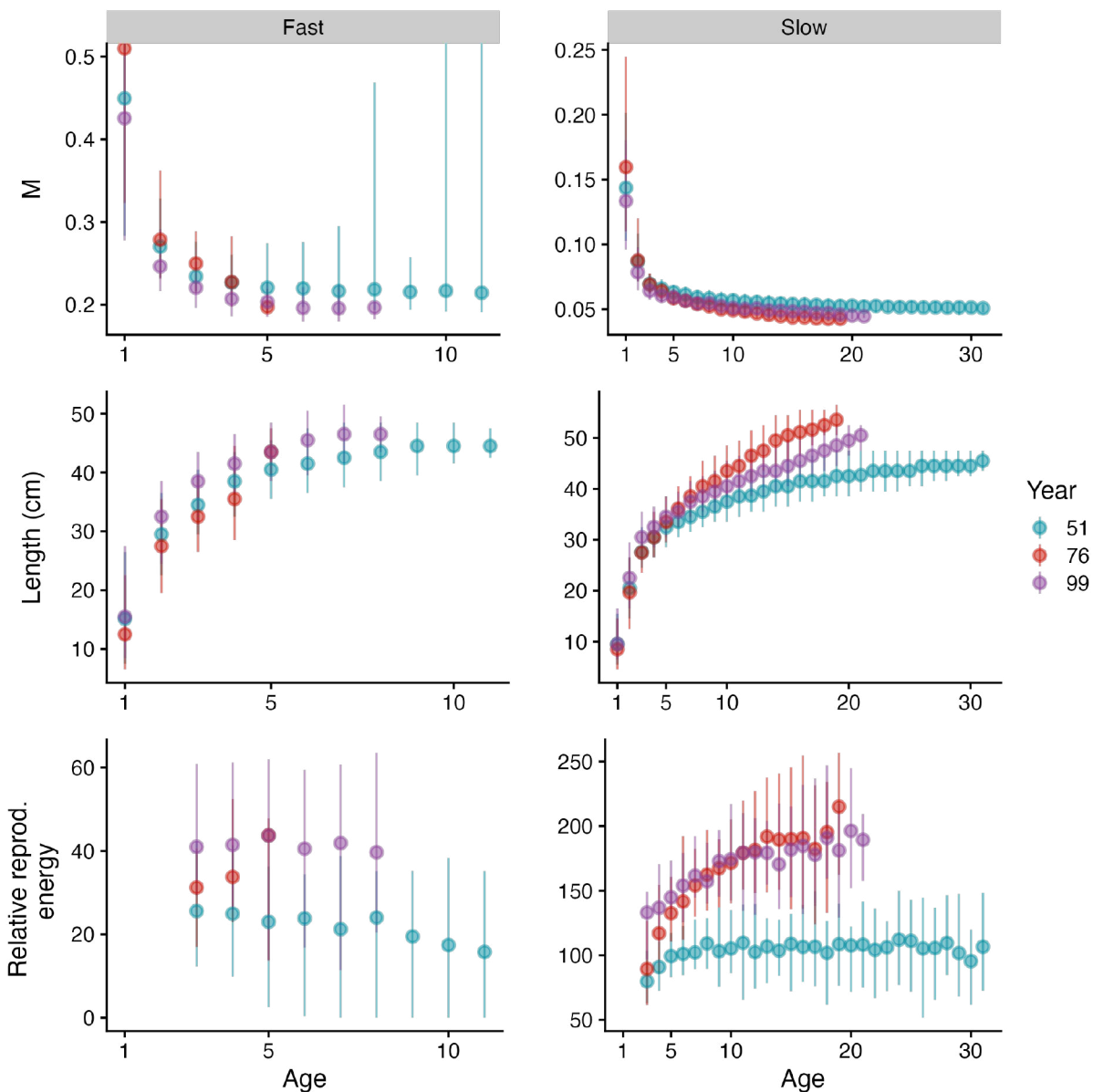


Figure B-4: Simulated values for productivity parameters for a single replicate (shown as red line in 2) for the base environmental scenario (constant temperature, constant environment). All parameters are shown as abundance-at-size weighted means-at-age for fish stocks with fast (left column) and slow (right column) life histories at the beginning of fishing (year 51), halfway through the fishing history (year 76), and for the final fishing year (year 99). Parameters are: natural mortality (M), length-at-age (Length), and relative reproductive energy. The simulation applied constant catch.

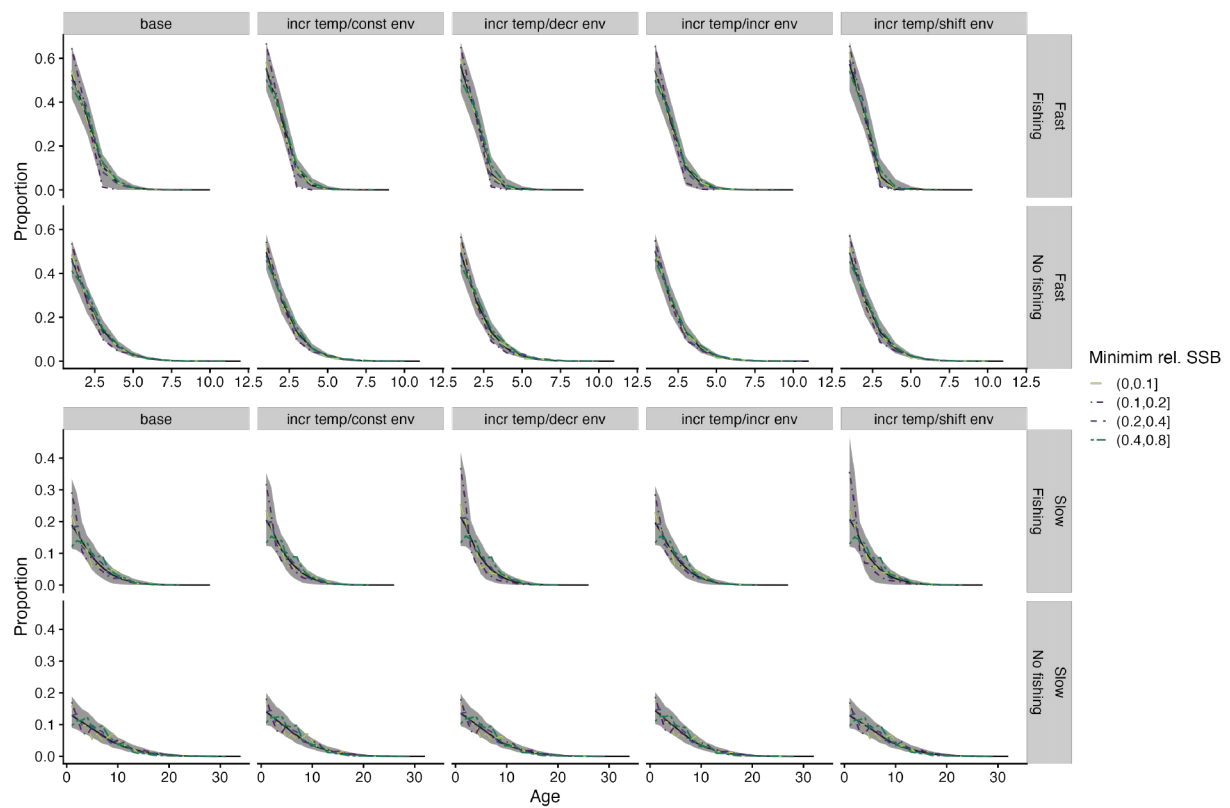


Figure B-5: Trajectories of simulated proportions-at-age in the final fishing year for fish stocks with fast (top two rows) and slow (bottom two rows) life histories, with catch constant. Shown are the median by year (black line) and the 95% inter-quantile range of simulations (grey shaded area) with proportions-at-age across all simulations, and randomly-selected simulation replicates (coloured and dashed lines). Simulations were with and without fishing for four different climate scenarios: base, no temperature or environmental change; incr temp/const env, increasing temperature, no environmental change; incr temp/decr env, increasing temperature, declining environment; incr temp/incr env, increasing temperature, increasing environmental suitability.

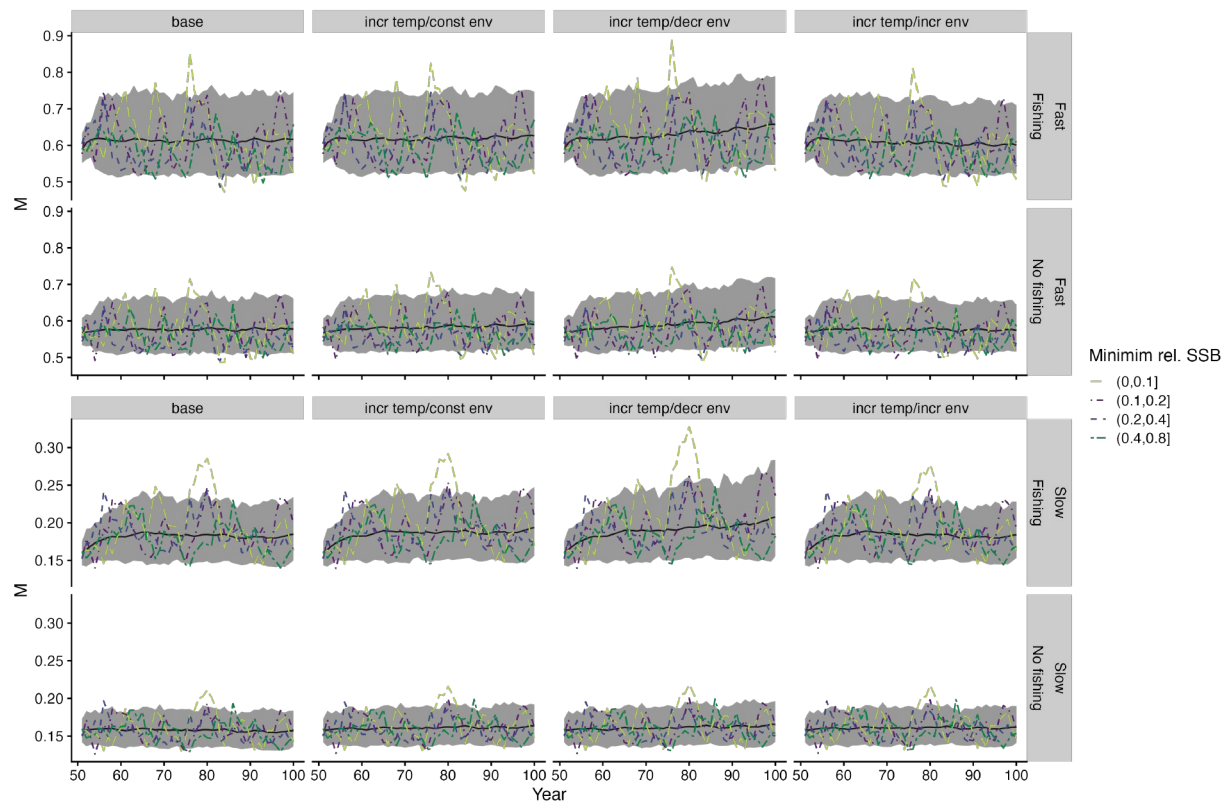


Figure B-6: Trajectories of simulated natural mortality M (abundance-weighted mean natural mortality) for fish stocks with fast (top two rows) and slow (bottom two rows) life histories, with catch constant. Shown are the median by year (black line) and the 95% inter-quantile range of simulations (grey shaded area) with M across all simulations, and randomly-selected simulation replicates (coloured and dashed lines). Simulations were with and without fishing for four different climate scenarios: base, no temperature or environmental change; incr temp/const env, increasing temperature, no environmental change; incr temp/decr env, increasing temperature, declining environment; incr temp/incre env, increasing temperature, increasing environmental suitability.

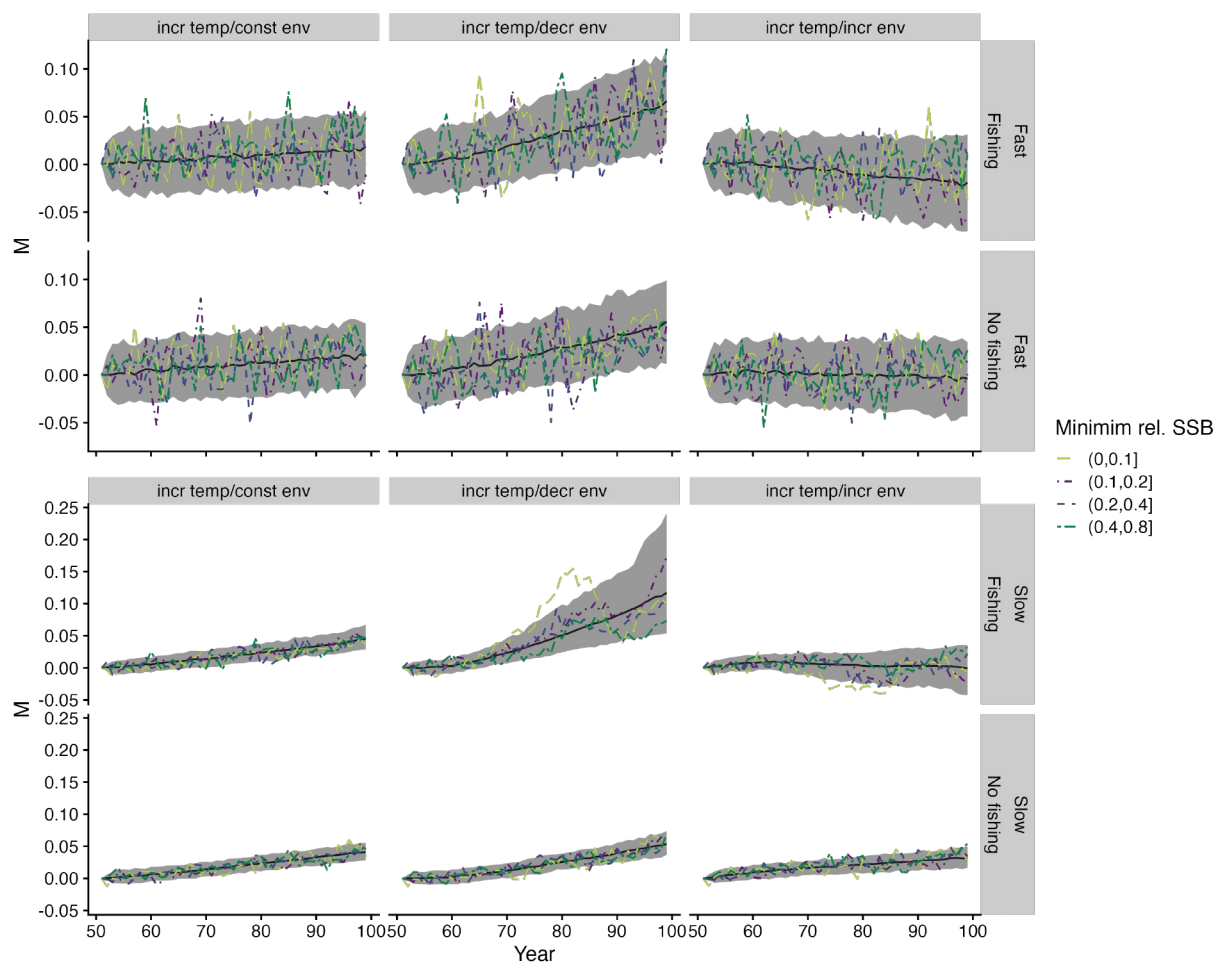


Figure B-7: Trajectories of relative natural mortality M (abundance-weighted mean natural mortality) relative to the base scenario for fish stocks with fast (top two rows) and slow (bottom two rows) life histories, with catch constant. Shown are the median by year (black line) and the 95% inter-quartile range of simulations (grey shaded area) with M across all simulations, and randomly-selected simulation replicates (coloured and dashed lines). Simulations were with and without fishing for three different climate scenarios, relative to the base scenario (no temperature or environmental change): incr temp/const env, increasing temperature, no environmental change; incr temp/decr env, increasing temperature, declining environment; incr temp/incre env, increasing temperature, increasing environmental suitability.

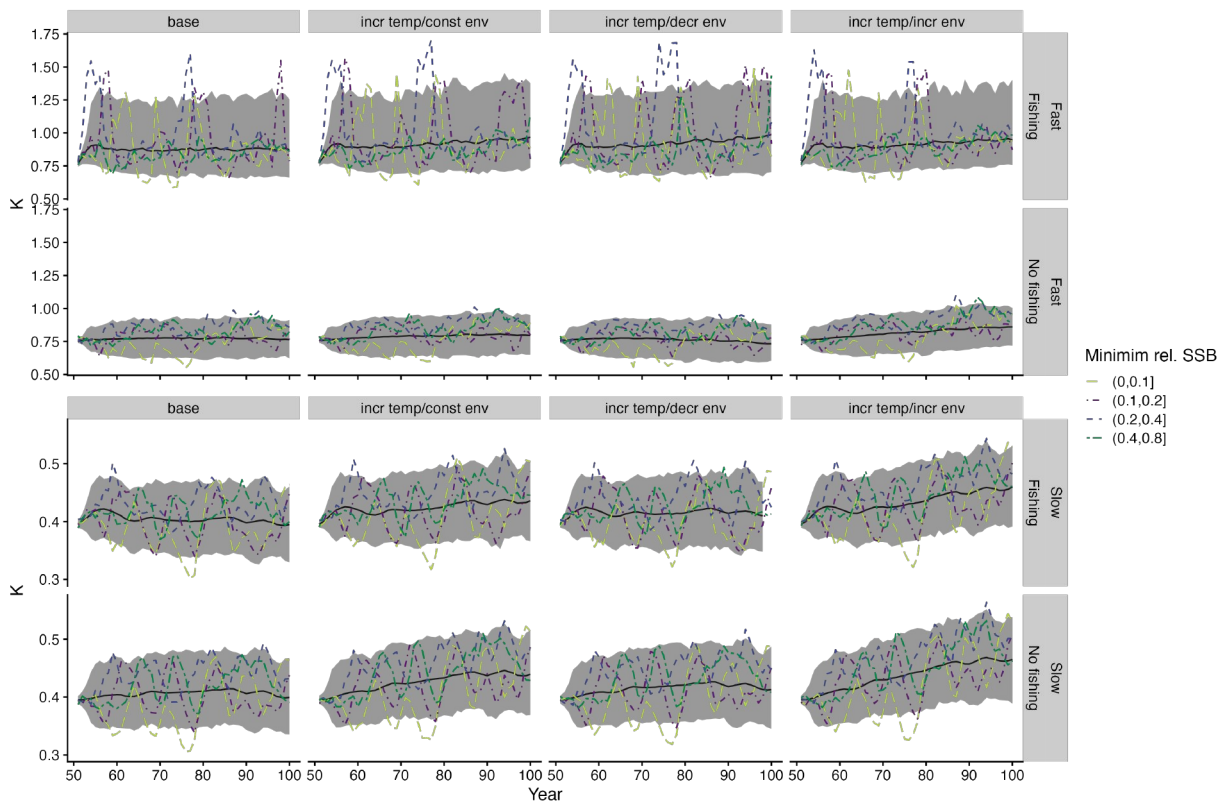


Figure B-8: Trajectories of simulated von Bertalanffy growth rate K (estimated from length-at-age for each year) for fish stocks with fast (top two rows) and slow (bottom two rows) life histories across all simulations, with fishing mortality constant. Shown are the median by year (black line) and the 95% inter-quartile range of simulations (grey shaded area) with K across all simulations, and randomly-selected simulation replicates (coloured and dashed lines). Simulations were with and without fishing for four different climate scenarios: base, no temperature or environmental change; incr temp/const env, increasing temperature, no environmental change; incr temp/decr env, increasing temperature, declining environment; incr temp/incre env, increasing temperature, increasing environmental suitability.

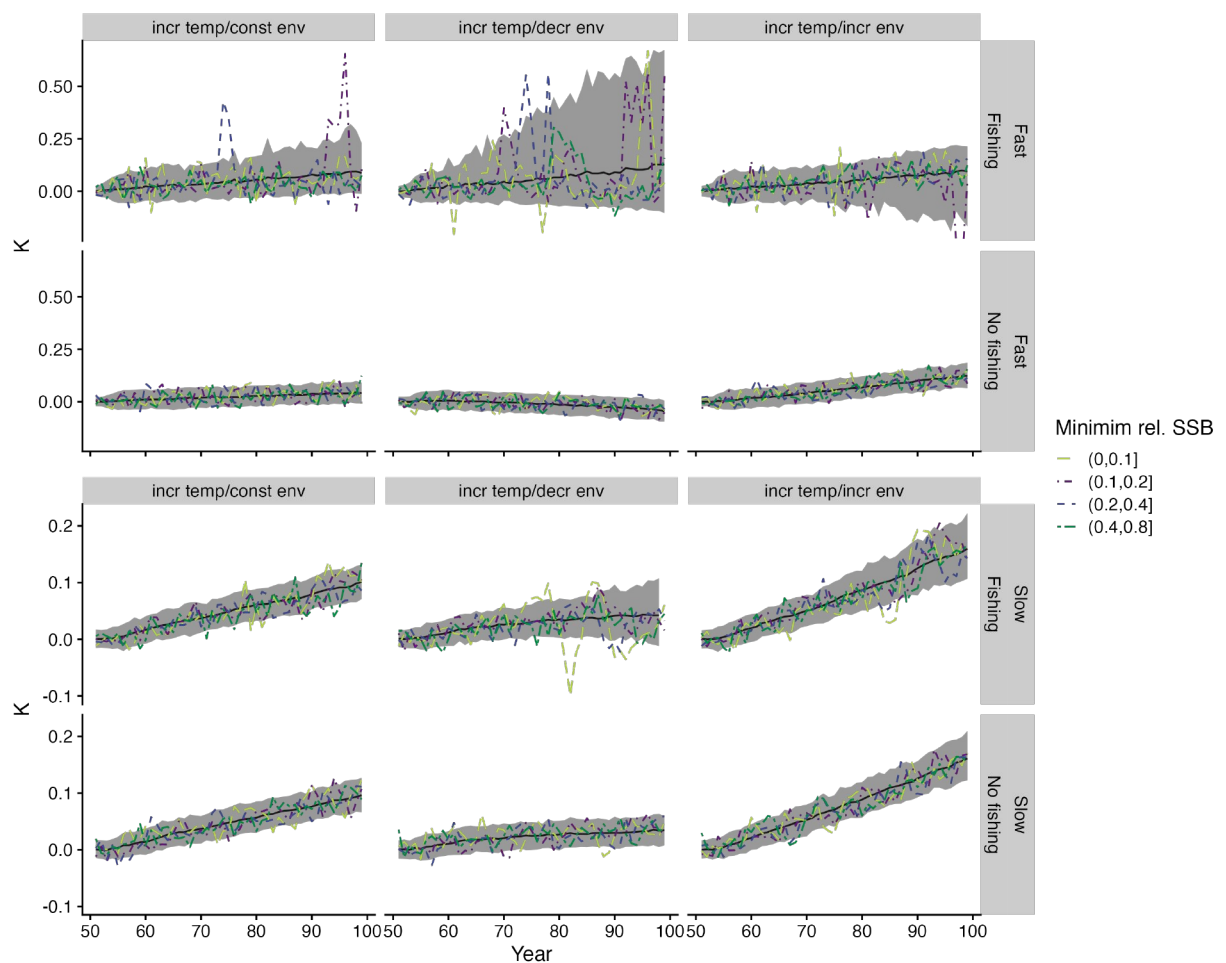


Figure B-9: Trajectories of relative von Bertalanffy growth rate K (estimated from length-at-age for each year) relative to the base scenario for fish stocks with fast (top two rows) and slow (bottom two rows) life histories, with catch constant. Shown are the median by year (black line) and the 95% inter-quantile range of simulations (grey shaded area) with K across all simulations, and randomly-selected simulation replicates (coloured and dashed lines). Simulations were with and without fishing for three different climate scenarios, relative to the base scenario (no temperature or environmental change): incr temp/const env, increasing temperature, no environmental change; incr temp/decr env, increasing temperature, declining environment; incr temp/incr env, increasing temperature, increasing environmental suitability.

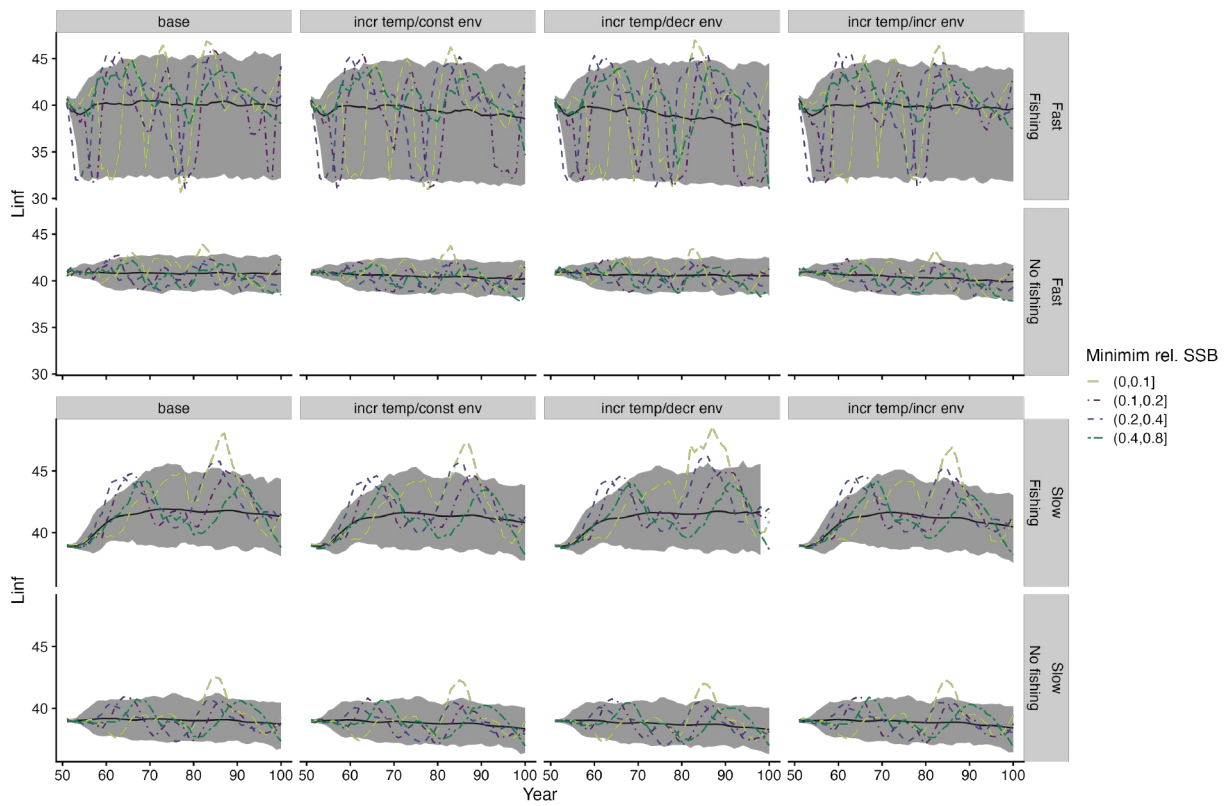


Figure B-10: Trajectories of simulated asymptotic fish size L_∞ (estimated by fitting von Bertalanffy growth curves from length-at-age for each year) for fish stocks with fast (top two rows) and slow (bottom two rows) life histories, with catch constant. Shown are the median by year (black line) and the 95% inter-quantile range of simulations (grey shaded area) with L_∞ across all simulations, and randomly-selected simulation replicates (coloured and dashed lines). Simulations were with and without fishing for four different climate scenarios: base, no temperature or environmental change; incr temp/const env, increasing temperature, no environmental change; incr temp/decr env, increasing temperature, declining environment; incr temp/incr env, increasing temperature, increasing environmental suitability.

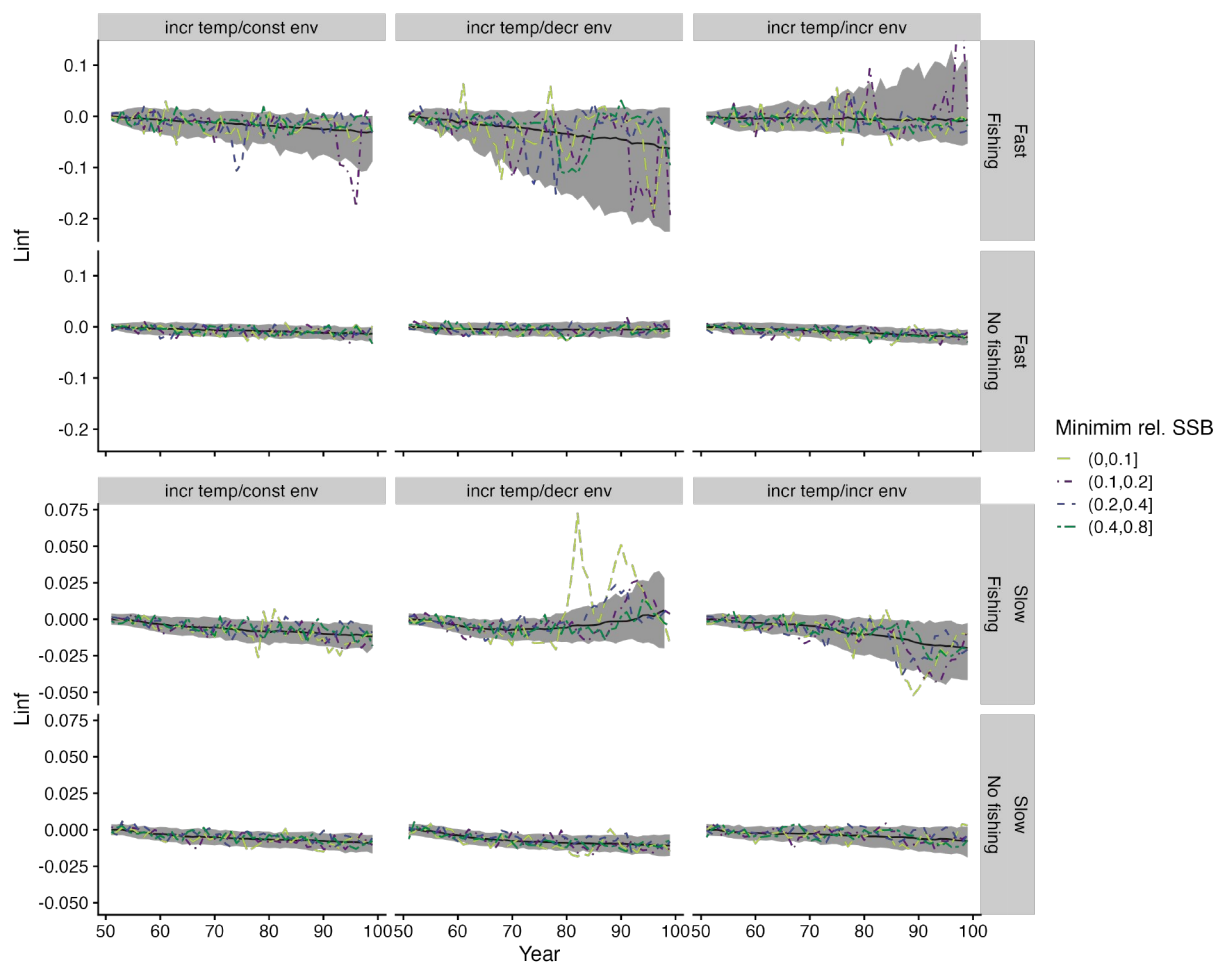


Figure B-11: Trajectories of relative asymptotic fish size L_{∞} (estimated by fitting von Bertalanffy growth curves from length-at-age for each year) relative to the base scenario for fish stocks with fast (top two rows) and slow (bottom two rows) life histories, with catch constant. Shown are the median by year (black line) and the 95% inter-quantile range of simulations (grey shaded area) with L_{∞} across all simulations, and randomly-selected simulation replicates (coloured and dashed lines). Simulations were with and without fishing for three different climate scenarios, relative to the base scenario (no temperature or environmental change): incr temp/const env, increasing temperature, no environmental change; incr temp/decr env, increasing temperature, declining environment; incr temp/incr env, increasing temperature, increasing environmental suitability.

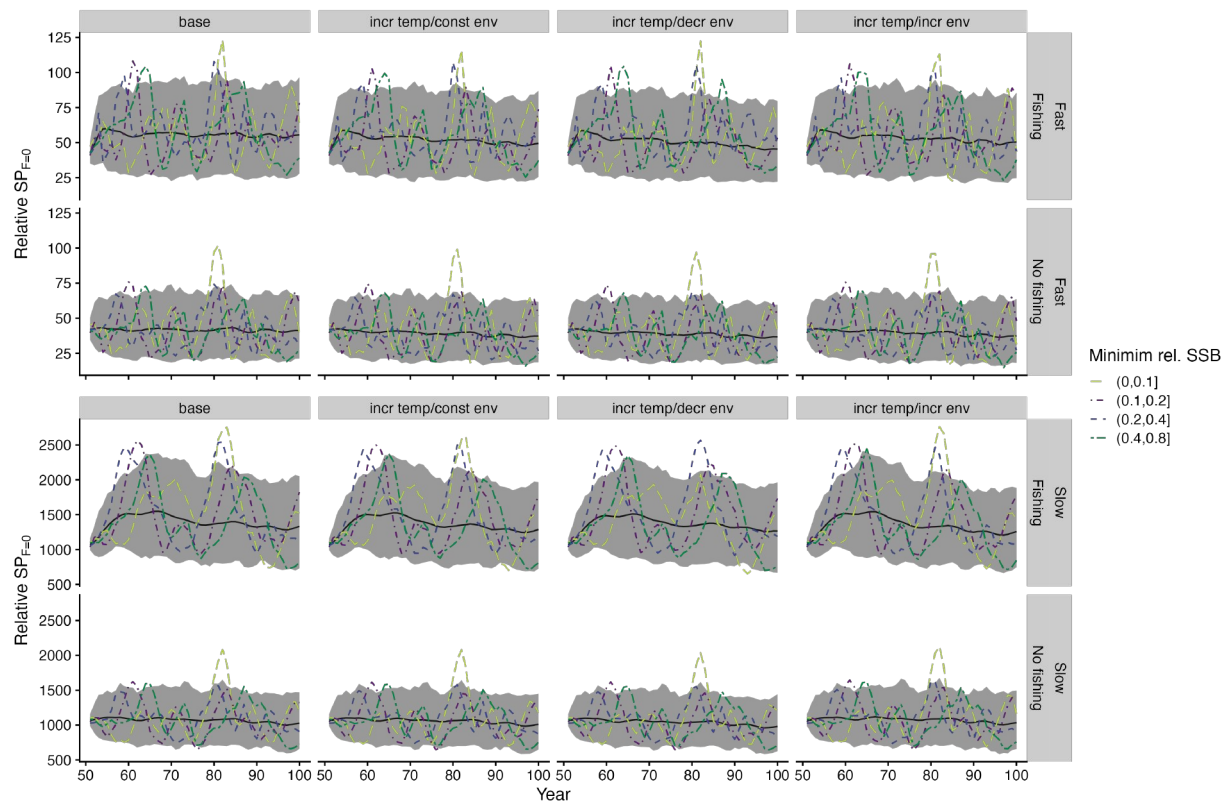


Figure B-12: Trajectories of instantaneous spawning potential without fishing $SP_{F=0}$ (calculated taking annually-realised productivity parameter values across age classes present in that year) for fish stocks with fast (top two rows) and slow (bottom two rows) life histories, with catch constant. Shown are the median by year (black line) and the 95% inter-quartile range of simulations (grey shaded area) with $SP_{F=0}$ across all simulations, and randomly-selected simulation replicates (coloured and dashed lines). Simulations were with and without fishing for four different climate scenarios: base, no temperature or environmental change; incr temp/const env, increasing temperature, no environmental change; incr temp/decr env, increasing temperature, declining environment; incr temp/incre env, increasing temperature, increasing environmental suitability.

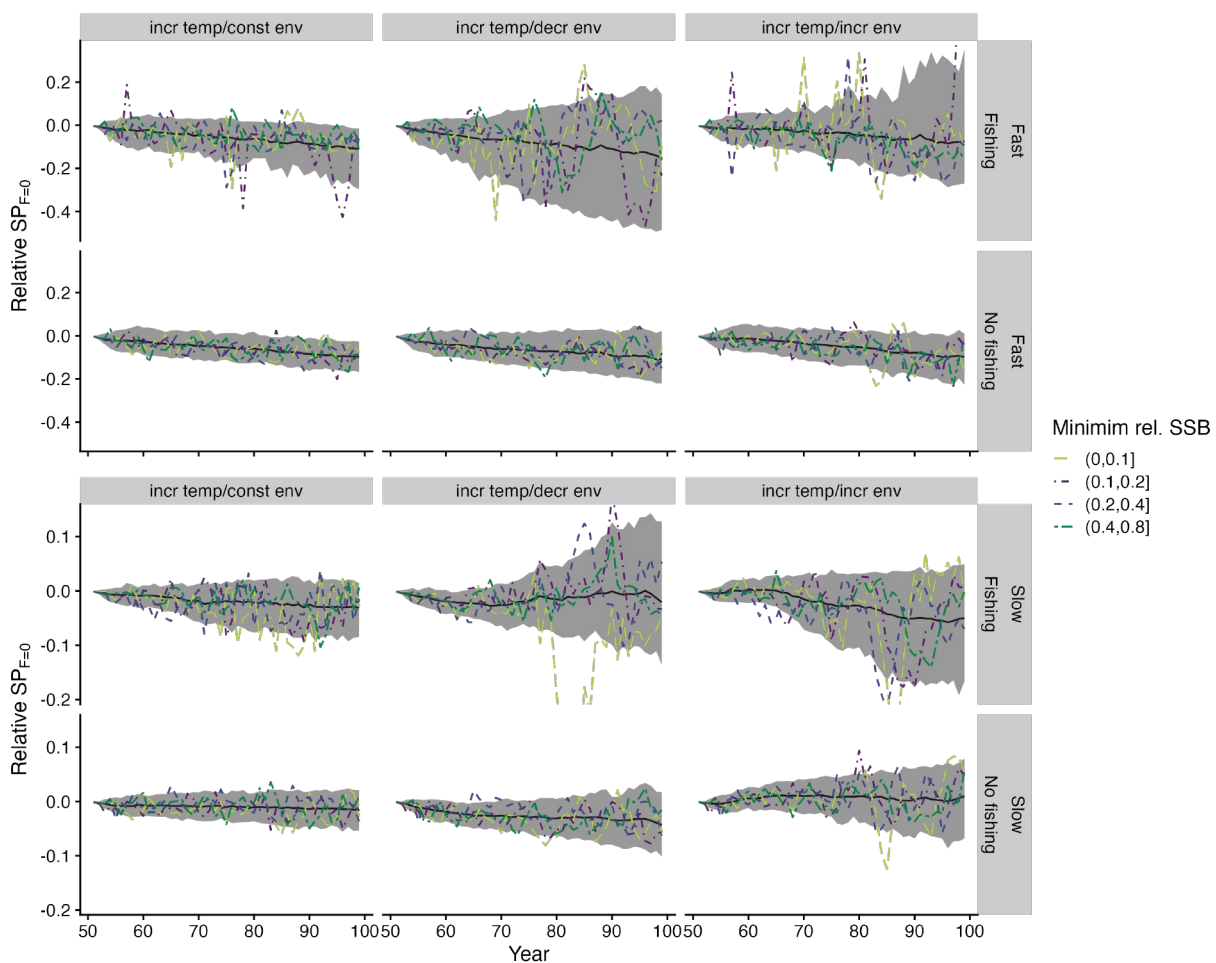


Figure B-13: Trajectories of relative instantaneous spawning potential without fishing $SP_{F=0}$ (calculated taking annually-realised productivity parameter values across age classes present in that year) relative to the base scenario for fish stocks with fast (top two rows) and slow (bottom two rows) life histories, with catch constant. Shown are the median by year (black line) and the 95% inter-quantile range of simulations (grey shaded area) with $SP_{F=0}$ across all simulations, and randomly-selected simulation replicates (coloured and dashed lines). Simulations were with and without fishing for three different climate scenarios, relative to the base scenario (no temperature or environmental change): incr temp/const env, increasing temperature, no environmental change; incr temp/decr env, increasing temperature, declining environment; incr temp/incr env, increasing temperature, increasing environmental suitability.

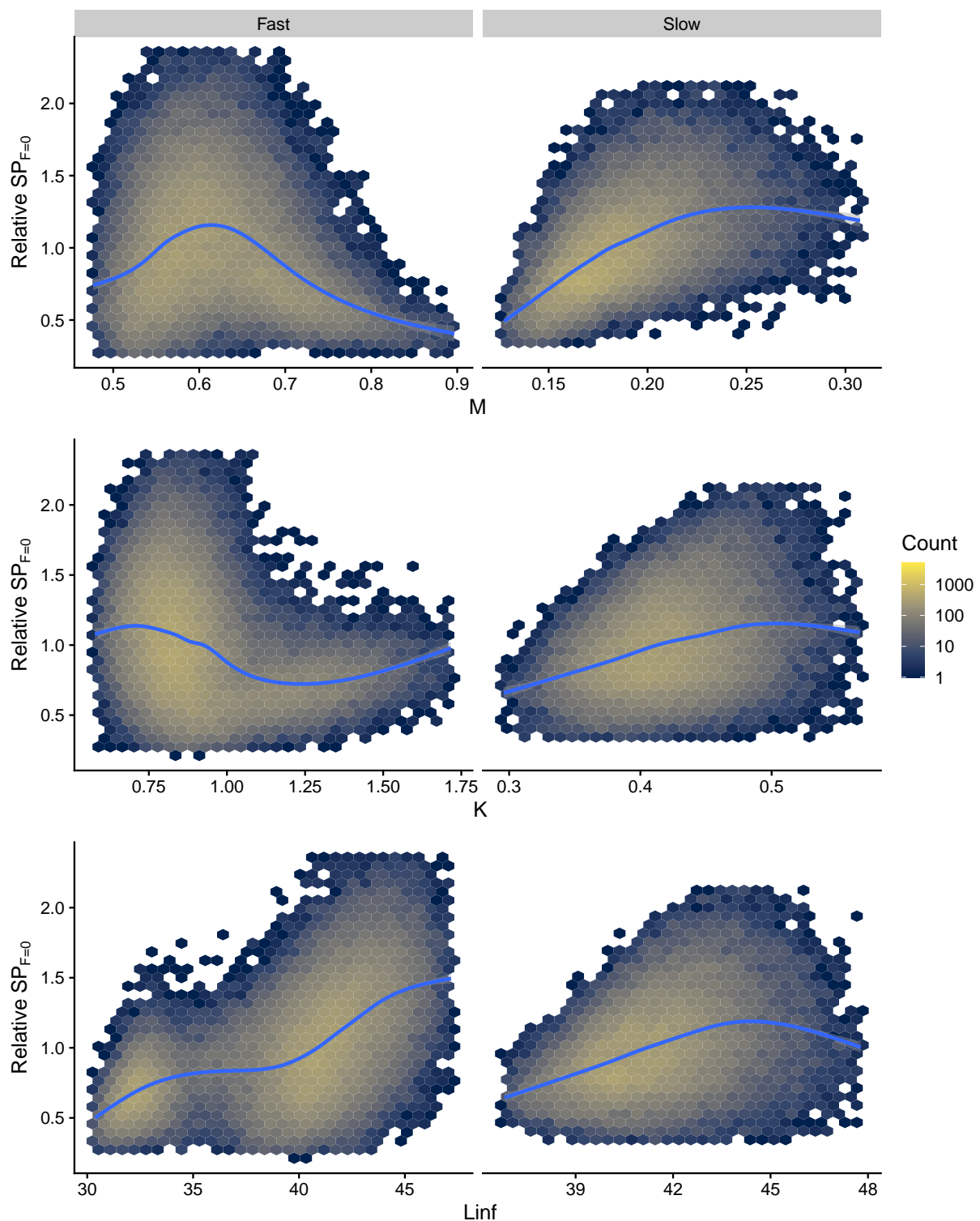


Figure B-14: Correlation between spawning potential without fishing $SP_{F=0}$ (calculated taking annually-realised productivity parameter values across age classes present in that year) and individual productivity parameters in the model for simulations with constant catch. Production parameters were: M , natural mortality; K , von Bertalanffy growth rate; L_{∞} (L_{inf}), asymptotic fish size.